

1
2
3
4
5
6
7
8
9
10
11
12
13
14
15
16
17
18
19
20
21
22
23
24
25
26
27
28
29
30
31
32
33
34
35
36
37
38
39
40
41
42
43
44
45
46
47
48
49
50
51
52
53
54
55
56
57
58
59
60

1 The Structure and Petrology of the Cnoc nan Cuilean 2 Intrusion, Loch Loyal Syenite Complex, north-west Scotland

3
4 **H.S.R. Hughes^{1*}, K.M. Goodenough², A.S. Walters³, M. McCormac², A.G. Gunn³, A. Lacinska³**

5 ¹Cardiff University, School of Earth and Ocean Sciences, Main Building, Park Place, Cardiff CF10 3AT

6 ²British Geological Survey, Murchison House, West Mains Road, Edinburgh, EH9 3LA

7 ³British Geological Survey, Kingsley Dunham Centre, Keyworth, Nottingham, NG12 5GG

8 *Corresponding author: hughesh6@cardiff.ac.uk

9
10
11
12 *Category: Research paper*

13 *Short title: Petrology of the Cnoc nan Cuilean Intrusion*

14 *Words: 8513 (+ 913 in reference list)*

15 *References: 34*

16 *Figures: 11*

17
18 *Declaration of Interest: None. No conflicts of interest.*
19

1
2
3 20 **Abstract**
4
5

6 21 In NW Scotland, several alkaline intrusive complexes of Silurian age intrude the
7
8 22 Caledonian orogenic front. The most northerly is the Loch Loyal Syenite Complex, which is
9
10 23 divided into three separate intrusions (Ben Loyal, Beinn Stumanadh, and Cnoc nan
11
12 24 Cuilean). Mapping of the Cnoc nan Cuilean intrusion shows two main zones: a Mixed
13
14 25 Syenite Zone (MZ) and a Massive Leucosyenite Zone (LZ), with a gradational contact. The
15
16 26 MZ forms a lopolith, with multiple syenitic lithologies, including early basic melasyenites
17
18 27 and later felsic leucosyenites. Leucosyenite melts mixed and mingled with melasyenites,
19
20 28 resulting in extreme heterogeneity within the MZ. Continued felsic magmatism resulted in
21
22 29 formation of the relatively homogeneous LZ, invading western parts of the MZ and now
23
24 30 forming the topographically highest terrain. The identification of pegmatites,
25
26 31 microgranitic veins and unusual biotite-magnetite veins demonstrates the intrusion's
27
28 32 complex petrogenesis. Cross-sections have been used to create a novel 3D GoCad™ model
29
30 33 contributing to our understanding of the intrusion.
31
32
33
34
35
36

37 34 The Loch Loyal Syenite Complex is known to have relatively high concentrations of rare
38
39 35 earth elements (REE), and thus the area has potential economic and strategic value. At
40
41 36 Cnoc nan Cuilean, abundant REE-bearing allanite is present within melasyenites of the MZ.
42
43 37 Extensive hydrothermal alteration of melasyenites here formed steeply-dipping biotite–
44
45 38 magnetite veins, most enriched in allanite and other REE-bearing accessories. This study
46
47 39 has thus identified the area of greatest importance for further study of REE enrichment
48
49 40 processes in the Cnoc nan Cuilean intrusion.
50
51
52
53
54
55

56
57 42 **Keywords:** *Sutherland, Caledonian, REE, allanite, indigenous resources.*
58
59
60

43 1. Introduction

44 During the Ordovician to Silurian closure of the Iapetus Ocean, continental basement and
45 overlying sediments were deformed and metamorphosed during oblique collision of the
46 Laurentia, Baltica, and Eastern Avalonia continental blocks (Soper *et al.*, 1992; Torsvik *et al.*,
47 1996; McKerrow *et al.*, 2000; Dewey & Strachan, 2003). The resulting Caledonian orogenic
48 belt extends from Scandinavia and East Greenland, through the British Isles and beyond to
49 the Appalachians of North America. Scotland and Ireland (within Laurentia) underwent an
50 early orogenic phase, the Grampian arc-continent collision, with later Silurian Baltica-
51 Laurentia-Avalonia collision known as the Scandian event (c.435-425 Ma) (Coward, 1990).
52 Caledonian deformation within the NW Highlands was due to this Scandian event. In the
53 Northern Highlands of Scotland, the Caledonian belt is sharply delineated by the Moine
54 Thrust Zone (extending from Loch Eriboll to the Sound of Iona). To the east of this feature
55 the Caledonides comprise Neoproterozoic metasedimentary rocks of the Moine Supergroup
56 (including the Loch Eil, East Moine, and Morar Groups) with some inliers of basement
57 gneiss. To the west, Archaean gneisses of the Lewisian Gneiss Complex, overlain by
58 unmetamorphosed Neoproterozoic and Cambro-Ordovician strata, form a stable foreland
59 block (Johnstone and Mykura, 1989).

60 During the Scandian event, numerous magmatic intrusions were emplaced along the Moine
61 Thrust Zone. These are predominantly alkaline in composition, and range from mafic and
62 ultramafic early phases, to diorites and high Ba-Sr granites and syenites (Thompson &
63 Fowler, 1986; Tarney & Jones, 1994; Fowler & Henney, 1996; Fowler *et al.*, 2008). The most
64 northerly, and youngest, of these intrusions is the late-tectonic Loch Loyal Syenite Complex
65 (Parsons, 1999) – Figure 1. In this paper we present detailed mapping, petrological study

1
2
3 66 and three-dimensional modelling of the Cnoc nan Cuilean intrusion, the smallest body
4
5 67 within the Loch Loyal Syenite Complex, which has been little studied since the work of King
6
7 68 (1942). The Cnoc nan Cuilean intrusion is of particular interest at the present time for its
8
9 69 notably high rare earth element (REE) contents (Shaw & Gunn, 1993) and our work
10
11 70 investigates how these elements are concentrated within different zones of the intrusion. A
12
13 71 new approach for 3D modelling of an igneous intrusion has aided interpretations of its
14
15 72 structure, petrogenesis, and REE metallogenesis.
16
17
18
19

20 73 *(Insert Figure 1)*
21
22

23 74 **2. Regional setting**

24
25
26 75 The NW Highlands alkaline plutons are part of a wider suite of high Ba-Sr plutons that occur
27
28 76 across the Northern Highlands (Tarney & Jones, 1994). Petrographically these igneous
29
30 77 complexes can be divided into a western zone (syenite-dominated complexes e.g. Glen
31
32 78 Dessarry, Loch Loyal, Loch Borralan, and Loch Ailsh) and an eastern zone (e.g. the granite-
33
34 79 dominated suites of Strontian, Rogart, Helmsdale, Cluanie, and Strath Halladale) (Fowler *et*
35
36 80 *al.*, 2008). Of the alkaline magmas, the Loch Loyal Syenite Complex is dominated by quartz
37
38 81 syenites, whereas the Loch Ailsh and Loch Borralan plutons show a wider range of
39
40 82 compositions, including undersaturated syenites. It is thus likely that more than one
41
42 83 magmatic source is represented by these plutons (Parsons, 1972).
43
44
45
46
47

48
49 84 Recent work on the high Ba-Sr granites and syenites of the NW Highlands has led to the
50
51 85 recognition of the Caledonian Parental Magma Array (Fowler *et al.*, 2008). This
52
53 86 incorporated a range of magma sources formed by metasomatism of the mantle wedge by
54
55 87 various fluids, including those from subducted pelagic carbonates as well as the down-going
56
57
58
59
60

1
2
3 88 slab. Differentiation of magmatic products from the Caledonian Parental Magma Array via
4
5 89 fractional crystallisation and concurrent small magma batch assimilation ultimately led to
6
7
8 90 the extensive array of intrusion compositions observed throughout this region. Minor
9
10 91 country rock contamination is thought to have occurred throughout this process, affecting
11
12 92 the geochemistry of individual intrusions (Fowler, 1988; Fowler, 1992; Fowler *et al.*, 2008).
13
14

15 93 The Loch Loyal Syenite Complex is part of the NW Highlands alkaline plutonic suite,
16
17 94 comprising volumetrically small yet highly variable alkaline intrusions of Caledonian age that
18
19
20 95 occur along, and on both sides of, the Moine Thrust Zone. This suite also includes intrusions
21
22 96 at Loch Borralan and Loch Ailsh in Assynt (Johnstone & Mykura, 1989; Parsons, 1999;
23
24 97 Atherton & Ghani, 2002; Fowler *et al.*, 2008; Goodenough *et al.*, 2011). These magmatic
25
26 98 events were related to the subduction of Iapetus oceanic crust below Laurentia, resulting in
27
28 99 the production of ultramafic, mafic, granitic, and syenitic magmas (Thompson & Fowler,
29
30 100 1986; Fowler *et al.*, 2001; Atherton & Ghani, 2002; Fowler *et al.*, 2008). Thus there is an
31
32 101 association between strongly alkaline magmas and a zone of active crustal shortening,
33
34 102 rather than extension, in the NW Highlands (Goodenough *et al.*, 2004). This magmatism
35
36 103 occurred during and immediately after the Scandian collisional event at 435-425 Ma
37
38 104 (Goodenough *et al.*, 2011).
39
40
41
42
43

44 105 The ages of the alkaline intrusions have been used to constrain the timing of regional
45
46 106 deformation and development of the Moine Thrust Zone (Halliday *et al.*, 1987; Goodenough
47
48 107 *et al.*, 2011). An early magmatic pulse in the Assynt area was emplaced syn-tectonically at
49
50 108 430.7 ± 0.5 Ma, and was followed by the post-tectonic late suite of the Loch Borralan Pluton
51
52 109 at 429.2 ± 0.5 Ma (Goodenough *et al.*, 2011). Zircons from the Cnoc nan Cuilean syenites
53
54 110 have been dated at 426 ± 9 Ma (Halliday *et al.*, 1987) assumed to be a representative age for
55
56
57
58
59
60

1
2
3 111 all Loch Loyal Syenite Complex intrusions. More recent attempts at $^{206}\text{Pb}/^{238}\text{U}$ zircon dating
4
5 112 of Cnoc nan Cuilean have suggested an approximate age of 425 Ma. However, the majority
6
7 113 of zircons indicate the presence of inherited age components from 1000–2500 Ma
8
9 114 (Goodenough *et al.*, 2011). The age of the Loch Loyal Syenite Complex is thus within error of
10
11 115 the only other post-tectonic alkaline intrusion in the NW Highlands (the late suite of the
12
13 116 Loch Borralan Pluton).
14
15
16

17
18 117 The Loch Loyal Syenite Complex is situated in the Tongue district of NW Scotland
19
20 118 (Holdsworth *et al.*, 2001) to the east of the Moine Thrust Zone (Fig. 1). The country rocks in
21
22 119 this area are chiefly metasedimentary rocks of the Neoproterozoic Moine Supergroup, with
23
24 120 some inliers of amphibolite-facies basement gneiss that show similarities to the Lewisian
25
26 121 Gneiss Complex of the Caledonian foreland and are termed ‘Lewisianoid’ (Tanner, 1970;
27
28 122 Moorhouse & Moorhouse, 1977). The Moine rocks of this area belong entirely to the basal
29
30 123 Morar Group of the Moine Supergroup, and comprise greenschist to amphibolite facies
31
32 124 psammites and pelites. During the Scandian orogenic event these rocks were
33
34 125 metamorphosed, folded, and thrust WNW over the Caledonian Foreland along the Moine
35
36 126 Thrust.
37
38
39
40
41

42 127 The Loch Loyal Syenite Complex consists of three syenitic masses (Fig. 2) – the Ben Loyal,
43
44 128 Cnoc nan Cuilean, and Beinn Stumanadh intrusions (Read, 1931; King, 1942; Robertson &
45
46 129 Parsons, 1974; Johnstone & Mykura, 1989). It represents the largest area of alkaline rocks in
47
48 130 the UK (Parsons, 1999). The Loch Loyal Syenite Complex lies within late Caledonian large
49
50 131 cross-folds (Fig. 2) resulting in NW–SE trending country rock foliation, oblique to the
51
52 132 region’s NNE–SSW orogenic strike (McErlean *et al.*, 1992; Holdsworth *et al.*, 1999). This zone
53
54
55 133 of folding is underlain by the ESE-dipping Ben Blandy shear zone. There is little evidence of
56
57
58
59
60

1
2
3 134 country rock deformation as a direct result of the syenite intrusion. However, limited top-to-
4
5 135 the-southeast extension may have occurred on the NW margin of the Ben Loyal intrusion.
6
7
8 136 This indicates that the overall geometry of the Loch Loyal Syenite Complex intrusions has
9
10 137 been controlled primarily by the pre-existing country rock structures into which they were
11
12 138 intruded (Holdsworth *et al.*, 1999). Throughout the region Caledonian compressional
13
14
15 139 features are post-dated by a series of low-angle faults, probably the result of late-orogenic
16
17 140 extension of the Caledonian nappe pile (Holdsworth *et al.*, 2001).

18
19
20 141 The largest intrusion within the complex, Ben Loyal, is separated from the Beinn Stumanadh
21
22 142 and Cnoc nan Cuilean intrusions by the Loch Loyal Fault, a major NE-SW trending dextral
23
24
25 143 oblique fault (Holdsworth *et al.*, 2001). It has been suggested that the Ben Loyal intrusion
26
27 144 may represent a deeper erosion level, and Beinn Stumanadh and Cnoc nan Cuilean the
28
29 145 upper sheeted levels (Holdsworth *et al.*, 1999). However, the Cnoc nan Cuilean intrusion (c.3
30
31 146 km²) is significantly chemically different to the Ben Loyal syenites (Parsons, 1999). This
32
33 147 contrast is further accentuated by the heterogeneous nature of Cnoc nan Cuilean rocks
34
35 148 (King, 1942; Gallon, 1974). The shape of the intrusion has been debated in the past, with
36
37 149 suggestions of a rounded outline (King, 1942), a squat ellipsoid (Gallon, 1974) or a series of
38
39 150 NW-trending dykes (Holdsworth *et al.*, 2001).

40
41
42
43
44 151 Prior to this investigation, little detailed work had been carried out across the Cnoc nan
45
46 152 Cuilean intrusion, with early study identifying essentially two broad zones. A relatively
47
48 153 homogeneous coarse-grained massive pink syenite in the centre of the intrusion was
49
50 154 separated from a structurally complex, heterogeneous 'variable syenite zone' forming the
51
52 155 lower marginal slopes of the intrusion (King, 1942). Mafic material within the mixed syenite
53
54 156 zone was originally considered to be country rock-derived (King, 1942). All syenites of this
55
56
57
58
59
60

1
2
3 157 intrusion have lower normative quartz contents, higher orthoclase, and are significantly
4
5 158 richer in clinopyroxene and amphibole (Parsons, 1999) than Ben Loyal lithologies. A
6
7 159 significant radiometric anomaly was also discovered over the eastern flank of the intrusion
8
9
10 160 due to high concentrations of thorite (Gallagher *et al.*, 1971). This paper presents new data
11
12 161 arising from mapping and petrographical study of the Cnoc nan Cuilean intrusion.

13
14
15
16 162 *(Insert Figure 2)*

17 18 19 163 **3. Field relationships at Cnoc nan Cuilean**

20
21 164 A new geological map for the Cnoc nan Cuilean intrusion is presented in Figure 3. On the
22
23 165 basis of new field data, the syenites of the Cnoc nan Cuilean intrusion are subdivided into
24
25 166 two main zones: a 'Mixed Syenite Zone' (MZ) and a 'Massive Leucosyenite Zone' (LZ) (Fig. 3).
26
27 167 Discrete episodes of later veining have also been identified. The LZ is defined as an area of
28
29 168 massive leucosyenite with less than 10% of the mafic melasyenite lithology. By contrast, the
30
31 169 MZ contains leucosyenite with abundant enclaves of melasyenite, country rock xenoliths
32
33 170 (with varying degrees of alteration and assimilation), and other mafic material. The
34
35 171 boundary between these zones is gradational (over approximately 50–100 m).
36
37
38

39
40
41 172 *(Insert Figure 3)*

42 43 44 173 **3.a. The Mixed Syenite Zone (MZ)**

45
46
47 174 The MZ, which occurs on the lower eastern and south-eastern slopes of Cnoc nan Cuilean
48
49 175 (Fig. 3), is a complicated zone that includes both melasyenitic and leucosyenitic lithologies,
50
51 176 as well as xenoliths of country rock. This zone is broadly similar to the 'Variable Marginal
52
53 177 Syenite' zone of King (1942). Leucosyenites are generally equigranular, medium- to coarse-
54
55 178 grained, and pinkish-white in colour. They comprise plagioclase, K-feldspar and minor
56
57
58
59
60

1
2
3 179 quartz, and black-greenish-brown pyroxene and amphibole, locally with coarse euhedral
4
5 180 titanite (with red-brown staining surrounding crystals). In contrast, the darker-coloured
6
7
8 181 melasyenites have higher modal proportions of pyroxene and amphibole (30-65% mafic
9
10 182 minerals), are equigranular (crystal sizes normally ranging up to 1 mm) and are generally
11
12 183 finer-grained than leucosyenites.

13
14
15 184 The two main lithologies show complex interrelationships, with examples of mingling (the
16
17 185 physical coexistence of the two liquids), veining, and a more gradational relationship
18
19 186 between the mela- and leucosyenites more indicative of magma mixing. Parts of the MZ
20
21 187 comprise veins of pink leucosyenite and microgranite cutting through massive melasyenite
22
23 188 and enclosing polygonal melasyenite enclaves, in some places resembling a stockwork. The
24
25 189 MZ melasyenite can appear as centimetre to metre-scale enclaves, or as more massive
26
27 190 bodies cut by a few veins of leucosyenite. Leucosyenite vein contacts here are generally
28
29 191 sharp (often with millimetre-scale clinopyroxene selvages) but some gradational contacts
30
31 192 (grading over 1-20mm) are encountered, often with wisps of leucosyenite fingering into
32
33 193 melasyenites, implying partial assimilation or mixing. Microgranite vein contacts with mela-
34
35 194 and leucosyenites are always sharp and well defined. Microgranite is distinguished from
36
37 195 leucosyenites by its lack of any mafic mineral phases, instead consisting of medium to
38
39 196 coarse grained quartz and feldspars only. In some areas, enclaves of melasyenite have
40
41 197 lobate contacts against the leucosyenites (Fig. 4a) that indicate extensive magma mingling.
42
43 198 Elsewhere, more gradational contacts are seen, indicating mixing resulting in chemical
44
45 199 interaction of the syenite magmas (Fig. 4b). Some larger bodies of melasyenite (up to c. 10
46
47 200 m wide) have little or no leucosyenite veining. Thus, within the MZ as a whole, there is
48
49 201 complete textural variation from angular, blocky melasyenite enclaves that were solid
50
51
52
53
54
55
56
57
58
59
60

1
2
3 202 before intrusion of the leucosyenites, through well-defined rounded melasyenite enclaves
4
5 203 with lobate contacts indicating physical mingling of two magmas, to blurred, gradational and
6
7 204 indistinct zones of chemical mixing between the two main magmas. It is evident that the
8
9 205 melasyenites pre-date the leucosyenites, but that the leucosyenites were intruded whilst
10
11 206 the melasyenite magmas were only partly crystallised. The field evidence for two co-existing
12
13 207 magmas indicates that the majority of the mafic material in the MZ was not derived from
14
15 208 the country rock, as originally suggested by King (1942). Similar features occur in the Loch
16
17 209 Ailsh pluton further south, where syenites cross-cut and enclose xenoliths of pyroxenite and
18
19 210 melasyenite (Parsons, 1968; Parsons, 1999). Xenoliths of country rock do also occur
20
21 211 throughout the MZ, and typically retain their original foliation.
22
23
24
25
26

27 212 *(Insert Figure 4)*
28
29

30 213 **3.b. The Massive Leucosyenite Zone (LZ)**

31
32
33 214 The LZ occurs towards the western edge of the intrusion and as the topographically higher
34
35 215 outcrops on Meall Eudainn and Creag nan Cat (Fig. 3). This zone comprises massive, coarse-
36
37 216 grained, pink, equigranular, pyroxene and hornblende-bearing leucosyenite. The LZ consists
38
39 217 mainly of the same type of leucosyenite as seen in the MZ, but here it accounts for more
40
41 218 than 90% of igneous lithologies present. Both here and in the MZ, finer-grained light-
42
43 219 coloured leucosyenite veins are observed cross-cutting the main leucosyenite (Fig. 4c).
44
45 220 Country rock xenoliths are also observed within this zone, although less commonly than in
46
47 221 the MZ. The LZ grades into the MZ over 50-100 metres, with gradually increasing amounts of
48
49 222 the melasyenite component as enclaves and larger bodies.
50
51
52
53
54

55 223 **3.c. Pegmatites and volatile-rich veining lithologies**

56
57
58
59
60

1
2
3 224 Syenitic pegmatites are commonly encountered in both the MZ and LZ, although pegmatites
4
5 225 only occur within leucosyenite of these zones (Fig. 4d) and not within melasyenite.
6
7 226 Pegmatite can occur as discrete pockets or veins generally < 20 cm wide and typically with
8
9 227 coarse hornblende- or clinopyroxene-rich selvages. The restriction of pegmatite to the
10
11 228 leucosyenite lithology suggests that a volatile-rich liquid stemmed from this later felsic
12
13 229 magma. Leucosyenite of the LZ contains variable patches of pegmatite, and in turn
14
15 230 pegmatite veins and lenses are cross-cut by later leucosyenite and microgranite veins.
16
17
18
19
20 231 Pyroxene- and allanite-rich stringers or veinlets are observed throughout the intrusion.
21
22 232 Veinlets are discontinuous, up to 5 mm wide, and cross-cut leucosyenites, melasyenites,
23
24 233 xenoliths, and biotite-rich inclusions. Pyroxene/allanite-rich stringers have also been
25
26 234 observed being cross-cut by microgranite veins in the Allt Liath stream section of the MZ
27
28 235 (Fig. 3). Therefore stringers are likely to have formed from a similar or the same volatile-rich
29
30 236 fraction as the pegmatites. In addition pegmatitic veins on the southern slopes of Meall
31
32 237 Eudainn contain clots of rhombic pyroxene.
33
34
35
36
37

38 **3.d. Microgranite veining**

39
40 239 Medium to coarse-grained, pink microgranite veins (containing abundant quartz and no
41
42 240 mafic minerals) cross-cut all other magmatic lithologies. This is thought to be the last
43
44 241 magmatic event within the intrusion. The veins are generally narrow (up to a few tens of
45
46 242 centimetres wide), discordant, and well defined with sharp, planar, intrusive margins.
47
48 243 Veining commonly offsets earlier syenites and pegmatite veins, or cross-cuts country rock
49
50 244 foliation. This is displayed at [NC 597465] where 10–40 cm wide bifurcating veins trend
51
52 245 almost perpendicular to Lewisianoid country rock banding.
53
54
55
56
57
58
59
60

1
2
3 246 **3.e. Biotite-magnetite alteration veins and areas of syenite alteration**
4

5
6 247 Allt Liath, on the eastern side of the Cnoc nan Cuilean intrusion, provides a c. 100 m east-
7
8 248 west trending section through the MZ. These exposures demonstrate a variety of textures
9
10 249 and cross-cutting relationships between all the magmatic lithologies, and provide evidence
11
12 250 for alteration of syenites by late fluids. Of particular interest are three highly friable,
13
14 251 approximately north-south trending vein systems composed primarily of vuggy or rounded
15
16 252 clots of magnetite and flaky biotite books (Fig. 4e). The locations and orientations of these
17
18 253 veins are indicated in Fig. 5.
19
20

21
22
23 254 These biotite-magnetite veins are up to 40 cm wide, steeply-dipping, sharply bounded, and
24
25 255 black in colour. They are characterised by high total radioactivity and locally high magnetic
26
27 256 susceptibility. The biotite-magnetite veins cross-cut all other igneous vein types and
28
29 257 syenites, with the exception of some pink microgranite veinlets (usually on the millimetre
30
31 258 scale but sometimes up to 10 cm wide) that anastomose within and across these alteration
32
33 259 zones. The biotite-magnetite vein infill observed in situ comprises a friable biotite and
34
35 260 magnetite 'matrix' with some more coherent blocks (up to fist-sized) of highly recrystallised,
36
37 261 but still recognisable, melasyenite. Thus the veins themselves are not deemed to be of
38
39 262 primary igneous origin; they appear to have been the result of intense syenitic alteration,
40
41 263 with the vein boundaries delineating the main pathway of late fluid.
42
43
44
45
46

47 264 Although biotite-magnetite vein contacts are clearly delineated visually by their black
48
49 265 colour, polygonal blocks of biotite-rich altered syenite up to tens of centimetres in size are
50
51 266 also common outside the biotite-magnetite vein margins within the immediately
52
53 267 surrounding leucosyenites of the Allt Liath stream section. These 'biotite-rich inclusions' are
54
55 268 characterised by coarse biotite crystals overprinting primary magmatic phases. Their field
56
57
58
59
60

1
2
3 269 relations indicate that these too are highly altered melasyenite blocks but appear distinct
4
5 270 from the main biotite-magnetite veins due to the possible splaying of these veins in three
6
7 271 dimensions. The MZ 'protolith' is very variable and it is possible that the leucosyenites of the
8
9 272 MZ were less dramatically altered due to their lower mafic mineral content, instead only
10
11 273 suffering feldspar seritisation and/or kaolinisation.
12
13
14

15 274 The biotite-magnetite veins formed late in the intrusion's history after the main syenites
16
17 275 had fully crystallised, and are the result of pervasive alteration by late-magmatic or
18
19 276 hydrothermal fluids. The late microgranite veins were unaffected by this fluid alteration,
20
21 277 but may have themselves been the source of the metasomatising fluids.
22
23
24

25
26 278 *(Insert Figure 5)*
27

28 29 279 **3.f. Country rocks and xenoliths** 30

31
32 280 Country rocks to the Cnoc nan Cuilean intrusion include both Moine and Lewisianoid
33
34 281 lithologies. Moine psammites are medium-grained, well-foliated, quartz-rich with varying
35
36 282 amounts of biotite. In contrast the Lewisianoid gneiss consists of banded hornblende
37
38 283 tonalite gneiss with some hornblende-rich mafic bands (or 'hornblendites').
39
40
41

42 284 Country rock xenoliths are common throughout the MZ, most particularly at marginal zones
43
44 285 [NC 614465] with both Moine and Lewisianoid examples at varying scales. In outcrop some
45
46 286 of these xenoliths clearly resemble the surrounding country rock with little or no evidence
47
48 287 of recrystallisation and alteration, often with leucosyenite or microgranite veining and relict
49
50 288 banding or folding. Some have sharp contacts, whereas in others the contacts are
51
52 289 gradational, indicating partial assimilation of the xenoliths by the surrounding magma.
53
54
55 290 However, some xenoliths are almost completely recrystallised, retaining their foliation but
56
57
58
59
60

1
2
3 291 with their mineralogy dominated by biotite (Fig. 4f). These are usually angular, with well-
4
5 292 defined and sharp contacts with the host syenite, however these xenoliths have been
6
7
8 293 metasomatised by potassic fluids, resulting in alteration to biotite.
9

10
11 294 In outcrop, Lewisianoid and Moine xenoliths typically occur either as discrete polygonal
12
13 295 blocks (up to a few tens of centimetres wide), or as metre-scale blocks fractured to form
14
15 296 mosaics of angular inclusions infilled by leucosyenite veining. Lozenge-shaped xenoliths with
16
17 297 narrow cross-cutting leucocratic veinlets (1–2 mm thick) are also observed in conjunction
18
19 298 with tightly crenulated xenoliths composed chiefly of coarse biotite and hornblende [NC
20
21 299 593463]. These probably originated from mafic bands within the Lewisianoid rocks. Source
22
23 300 Lewisianoid hornblendites do not contain biotite, but extensive alteration of xenoliths by
24
25 301 potassic fluids within the magma body could have led to this significant biotite overprinting.
26
27 302 Thus in combination with other clearly banded Lewisianoid xenoliths, evidence exists for a
28
29 303 continuum of xenolithic material varying between almost unaltered non-assimilated blocks
30
31 304 to completely metasomatised and replaced inclusions. Moine xenoliths are also observed,
32
33 305 displaying similar attributes to the Lewisianoid examples as regards their contacts, size,
34
35 306 veining, and alteration.
36
37
38
39
40
41

42 307 **3.g. Syenite, microgranite and country rock relationships at the intrusion margins**

43
44
45 308 The Moine and Lewisianoid country rocks are folded into an open, upright NW-plunging
46
47 309 synform in the immediate vicinity of the intrusion, within a series of major Caledonian cross-
48
49 310 folds (Holdsworth *et al.*, 1999; Holdsworth *et al.*, 2001).
50
51

52
53 311 Due to poor exposure, particularly at the margins of the Cnoc nan Cuilean intrusion, the
54
55 312 outline shape and contact orientations for the intrusion have been deduced from a few key
56
57
58
59
60

1
2
3 313 localities (as outlined below) and inferred from significant changes in topography around
4
5 314 the intrusion margins. Although when taken individually very few of these localities may
6
7 315 appreciably inform us of the overall shape of the intrusion, cumulatively these have proven
8
9 316 most instructive during the interpretation of field data and the construction of cross-
10
11 317 sections. Such localities tend to occur at similar topographic heights around the intrusion, in
12
13 318 concentrated zones of basal country rock xenoliths.
14
15
16
17

18 319 The NW margin of the intrusion shows a series of massive leucosyenite sheets intruding the
19
20 320 Lewisianoid gneisses parallel to their gneissose banding (Fig. 5 – map 1). Key localities
21
22 321 demonstrating this concordant relationship (where syenite veins intrude country rocks
23
24 322 parallel to their banding and foliation) occur at [NC 593464], [NC 594464], and [NC 595465].
25
26

27 323 At [NC 593464] highly crenulated biotite-rich Lewisianoid xenoliths can also be observed just
28
29 324 a few centimetres away from the leucosyenite/Lewisianoid contact. Rare examples of
30
31 325 discordant minor microgranite veins are also observed ([NC 595464] and [NC 598466]),
32
33 326 suggesting that this youngest magmatic episode did not necessarily conform to the overall
34
35 327 country rock structure to which the main intrusion is constrained.
36
37
38

39
40 328 The marginal zone of the intrusion around the stream of Allt Torr an Tairbh (NE margin – Fig.
41
42 329 5, Map 2) has a series of small exposures of Lewisianoid gneisses and Moine country rocks,
43
44 330 cut by microgranite veins (such as those seen between [NC 609470] and [NC 609471]) and
45
46 331 leucosyenite veins, ranging from centimetre-scale up to 5m thick, and extending northwards
47
48 332 from the lower MZ. Two larger sheets of mixed mela- and leucosyenites are seen from [NC
49
50 333 610471] to [NC 612472] inferred to be approximately 30 and 150m wide respectively
51
52 334 (although the syenite sheet/country rock contacts are not always visible) and interpreted as
53
54 335 northwards extensions of the lower MZ. Contacts between the Lewisianoid/Moine country
55
56
57
58
59
60

1
2
3 336 rocks and intrusive sheets are sharp, with little or no evidence of country rock melting and
4
5 337 no xenoliths observed. Grain size within these sheets is generally finer (< 1 mm) than the
6
7
8 338 main intrusion. This stream section provides a succession of contacts between intrusive
9
10 339 units and country rock, demonstrating that in this marginal zone, syenite sheets and
11
12 340 microgranite veins have been intruded as a series of concordant bodies (from centimetre to
13
14 341 metre-scale) parallel to Lewisianoid banding and Moine foliation (Fig. 5 – map 2).

15
16
17
18 342 No exposure of the intrusion margin exists in the area of Bealach na Beiste (SW intrusion
19
20 343 margin – Fig. 5 map 3) or along the lower ground on the south side of Meall Eudainn.
21
22 344 Therefore the contact marked on Figures 3 and 5 is inferred from a change in slope
23
24 345 approximately 500m SW of Lochan nan Cuilean, along with a single locality [NC 605452]
25
26 346 consisting of Moine country rock in contact with leucosyenite and cross-cut by numerous
27
28 347 narrow leucosyenite and microgranite veins (3-20 cm wide) discordant to Moine foliation.
29
30
31

32
33 348 On the eastern margin of the intrusion the change in hillside gradient below the crags west
34
35 349 and northwest of the Loch Loyal Lodge (Fig. 3) has been used to infer the location of the
36
37 350 intrusion/country rock contact. In addition craggy exposures such as those at [NC 615465]
38
39 351 show abundant tightly folded and/or foliated Lewisianoid xenoliths (up to 70cm long)
40
41 352 hosted and veined by leucosyenites. Numerous smaller-scale country rock xenoliths are
42
43 353 visible throughout this marginal section of the intrusion, associated with leucosyenite,
44
45 354 melasyenite, and pegmatites.
46
47
48
49

50 355
51
52

53 356
54
55
56
57
58
59
60

357 **4. 3D Modelling of the Pluton Geometry**

358 The Cnoc nan Cuilean intrusion is moderately well-exposed, but in many areas the contacts
359 are obscured by superficial deposits, and for this reason there has been debate about the
360 three-dimensional shape of the intrusion (e.g. Holdsworth et al., 1999). In order to
361 understand the extent of the MZ – and thus the potential scale of the REE-enriched area –
362 we have created a Paradigm GOCAD™ 3D model of the Cnoc nan Cuilean intrusion which
363 aids visualisation of the internal and external intrusive relationships. This is one of the first
364 instances that a 3D model has been used to help communicate a research study of a
365 complex igneous pluton in a scientific journal.

366 The model was built using GOCAD™ software (*Paradigm GOCAD™ 2009.3 Patch 3*) and
367 represents a rock volume approximately 9 km² in area and extending to approximately 200
368 metres below the topographic surface. The primary dataset consisted of a 3 by 4 rectilinear
369 grid of hand-drawn vertical structural cross-sections digitally captured in ESRI® ArcGIS™ (Fig.
370 6). Creating the model (Fig. 7) required several iterations, as the cross-sections that were
371 initially drawn on the basis of field relationships did not produce a reasonable 3D shape for
372 the intrusion. The cross-sections, and our understanding of the 3D size and shape of the
373 intrusion, thus evolved significantly during creation of the model, although always being tied
374 back to the primary field evidence at surface level.

375 **4.a. Summary of field evidence used in cross-section and model construction**

376 The overall surface outline of the LZ was based on the prevalence of massive leucosyenite
377 and absence of melasyenite on higher exposures of Meall Eudainn and Creag nan Cat. Based
378 on exposures at [NC 598457] and satellite imagery, two faults have been interpreted within

1
2
3 379 the intrusion (mapped as Faults 1 and 2). An elongate zone of massive leucosyenite,
4
5 380 exposed around Meall nan Eudainn and Creag nan Cat, extends along Fault 1 and is inferred
6
7 381 to have been the result of leucosyenite magma being fed along this fault. Thus cross-
8
9
10 382 sections 5, 6, and 7 (Fig. 6) document this leucosyenite body narrowing eastwards from
11
12 383 Cnoc nan Cuilean along Fault 1 and Creag nan Cat. In turn, a similar system along Fault 2
13
14 384 may go some way to explaining why a small zone of LZ can be observed to the north of the
15
16
17 385 intrusion at [NC 606467].
18
19

20 386 The steeper LZ sheets on the W of the intrusion (particularly around Cnoc nan Cuilean itself)
21
22 387 are seen in the field as previously described in Section 3.g. However, the detailed deeper
23
24 388 relationship between the MZ and LZ, as shown on the eastern side of cross-sections 3 and 4
25
26
27 389 (Fig. 6), is interpretive and based on the field evidence of surrounding country rock structure
28
29 390 (a northward plunging synform) which indicates that the MZ and LZ are generally
30
31 391 constrained to a lopolithic shape concordant with this structure. Therefore the later
32
33 392 introduction of massive leucosyenites to the earlier melasyenites resulted in the LZ fingering
34
35 393 into the MZ. These veining relationships internal to the intrusion are likely to be more
36
37 394 complicated than can be shown by this model, and those shown here are intended as
38
39 395 representative, to demonstrate the processes forming the intrusion.
40
41
42
43
44

45 396 *(Insert Figure 6)*
46
47

48 397 **4.b. The modelling process**

49
50

51 398 To create the model, the geo-referenced cross-section shapefiles were imported directly to
52
53 399 GOCAD™ along with the crop limit lines of the two syenite bodies (the MZ and LZ) and a set
54
55 400 of 10 m topographic contours. Shapefiles were converted within GOCAD™ to depth (Z)
56
57
58
59
60

1
2
3 401 attributed point sets, thereby providing a 'data cage' to constrain the model surface
4
5 402 geometry of the two syenite bodies. However, the intrusive surfaces proved problematic to
6
7 403 model directly from the cross-section data, as they were too widely spaced to define the
8
9 404 convoluted surface structure in 3 dimensions. To work around this, a stack of structure-
10
11 405 depth contours were constructed by linking matching elevation points on the cross-section
12
13 406 lines.

14
15
16
17
18 407 Approximations to the outer subsurface limits of the two syenite bodies were then created
19
20 408 by manual GOCAD™ surface construction functions, building the surface in upward steps
21
22 409 between adjacent depth contours. The resulting, approximately cylindrical, surface objects
23
24 410 were then fitted to the original cross-section line data using the GOCAD™ Discrete
25
26 411 Smoothing Interpolation algorithm (Mallet, 1997; Mallet, 2002). A smoothing and manual
27
28 412 surface edit operation was carried out to clean irregular artefacts and self-intersections in
29
30 413 the surface mesh and the modelled shape and extent of the major intrusive apophyses were
31
32 414 refined. It should be noted that many of the minor sheets, veins, and irregularities portrayed
33
34 415 on the cross-sections were at the limit of the practical resolution scale of the model and are
35
36 416 represented in simplified form. The top surface of the model intrusion, which corresponds
37
38 417 to the ground surface outcrop, was created separately from the Digital Terrain Model and
39
40 418 merged with the subsurface model surfaces.

41
42
43
44
45
46
47 419 *(Insert Figure 7)*

48 49 50 420 **4.c. Model results**

51
52
53 421 Figure 7 displays a variety of snapshot views from the final 3D model of the Cnoc nan
54
55 422 Cuilean intrusion. It demonstrates the saucer-shaped lopolith of the MZ (Fig. 7c) broadly

1
2
3 423 following the northward-plunging synformal structure of the Lewisianoid and Moine country
4
5 424 rocks (although these have not been included in the model for clarity). Through this initial
6
7 425 shallow intrusion, the LZ was intruded from a feeder zone located at the south-western or
8
9 426 western edge of the intrusion, with leucosyenitic magma becoming channelled along faults
10
11 427 within the intrusion (particularly Fault 1 trending NE-SW, Fig. 6). This resulted in the
12
13 428 elongated shape of the LZ in a NE direction (Fig. 7a). In addition, leucosyenites formed a
14
15 429 series of sheets approximately concordant to host Lewisianoid or Moine fabrics, as
16
17 430 displayed on the northern and NW sides of the intrusion, and best displayed by the
18
19 431 underside snapshot view of Figure 7b.
20
21
22
23
24

25 432 This 3D model is undoubtedly an interpretation, based on the observed field relationships
26
27 433 and our understanding of the processes that formed the Cnoc nan Cuilean intrusion. It is, of
28
29 434 course, constrained by only the available data from limited surface exposures. However, the
30
31 435 iterative process of building a 3D model has helped our understanding of the intrusion
32
33 436 shape to develop. We are confident that the model presented here provides a best estimate
34
35 437 of the 3D shape of the intrusion on the basis of the existing data, and it can be used as a
36
37 438 template for further investigation of Cnoc nan Cuilean.
38
39
40
41
42

43
44
45
46
47
48
49
50
51
52
53
54
55
56
57
58
59
60

440 **5. Petrology of intrusion lithologies**

441 **5.a. Melasyenite**

442 Melasyenites of the MZ comprise c. 45–60% feldspar and more than 30% mafic minerals.
443 Although the amount of mafic minerals is very variable, there is no systematic trend or
444 zonation across the intrusion. Most melasyenites are medium- to coarse-grained, but some

1
2
3 445 finer grained examples are encountered on the south side of Meall Eudainn and the east
4
5 446 side of Creag nan Cat. They are not porphyritic, but locally feldspars can be notably coarser
6
7 447 than mafic phases. Some are foliated, due to alignment of elongate pyroxenes.
8
9

10
11 448 Both plagioclase and K-feldspar are present in the melasyenite, but plagioclase is generally
12
13 449 less than 15% of the rock. K-feldspars are typically subhedral and interstitial to mafic
14
15 450 minerals and generally show perthitic exsolution lamellae. Quartz is present, but at less than
16
17 451 5%, and often has undulose extinction.
18
19

20
21 452 Mafic minerals include clinopyroxene (aegirine-augite to diopside), alkali amphibole and
22
23 453 titanite. Biotite does not occur as a primary magmatic phase, but patchy alteration of
24
25 454 syenites by late fluids is highlighted by the occurrence of tabular biotite crystals. Minor
26
27 455 magnetite flecks are observed, particularly as inclusions within clinopyroxene crystal rims.
28
29

30 456 Pyroxenes occur at much higher concentrations than amphiboles (usually > 3:1). Titanite,
31
32 457 commonly exceeding 5% content, occurs as euhedral rhombs up to 0.5 mm long, and is
33
34 458 frequently found clustered with clinopyroxene and apatite (Fig 9a). Generally, mafic
35
36 459 minerals often cluster together. Examples of both clinopyroxene with euhedral prismatic
37
38 460 titanite inclusions, and large subhedral titanites with rounded pyroxene inclusions are
39
40 461 observed. Pyroxene clusters may be rounded (sometimes in an orbicular texture) or as
41
42 462 stringers through the sample (Fig. 8a). One orbicular melasyenite (south Meall Eudainn)
43
44 463 shows individual rounded pyroxene crystals delineating the outer edge of the orbicules (Fig.
45
46 464 8b). The orbicule interiors contain similar shaped pyroxene crystals, titanite, and interstitial
47
48 465 K-feldspar. Coarse perthitic K-feldspar (and minor plagioclase) infills between the orbicules.
49
50 466 The origins of this texture are uncertain but they may have resulted from the replacement
51
52 467 of large primary rounded crystals, or have been formed during movement of crystal mush.
53
54
55
56
57
58
59
60

1
2
3 468 Rounded or granular, anhedral apatite crystals are common in melasyenites, often clustered
4
5 469 with pyroxenes or titanite. They often have a rim of allanite, are associated with more
6
7 470 blocky crystals of allanite, or have allanite infilling fractures (Fig. 8c). Allanite is also
8
9 471 observed as a late-magmatic phase interstitial to pyroxenes, titanite and apatite, or in veins
10
11 472 in some samples.
12
13
14

15 473 *(Insert Figure 8)*
16
17

18 474 **5.b. Leucosyenite**

19
20
21 475 The leucosyenites of Cnoc nan Cuilean are white-pink, generally unfoliated medium- to
22
23 476 coarse-grained massive syenites with less than 30% summed total of pyroxene, amphibole,
24
25 477 and titanite. Feldspars account for more than 50% of the leucosyenite, with higher
26
27 478 proportions of K-feldspar (perthite) than plagioclase. 5-15% quartz is generally present.
28
29 479 Allanite and apatite occur in markedly lower concentrations, with samples rarely displaying
30
31 480 the late-magmatic relationship of rounded apatite crystals rimmed by allanite. Allanite only
32
33 481 occurs as a rare fracture infill in some samples (predominantly from the Allt Liath area).
34
35
36
37
38

39 482 **5.c. Microgranite**

40
41
42 483 Microgranite occurs as veins throughout the Cnoc nan Cuilean intrusion, characterised by its
43
44 484 lack of mafic and accessory minerals. In rare cases mafic minerals are entrained from host
45
46 485 syenites. The microgranites are medium-grained, unfoliated and consist of equigranular
47
48 486 plagioclase, K-feldspar, and quartz. Plagioclase is the dominant feldspar (50–60%) with
49
50 487 lesser K-feldspar (c. 20%).
51
52
53
54
55
56
57
58
59
60

1
2
3 488 Some recrystallisation (typically associated with the introduction of biotite, allanite, or
4
5 489 clinopyroxene) occurs along the contacts of the microgranite veins with the mela- and
6
7 490 leucosyenites, indicating a higher volatile content within these younger granitic melts.
8
9

10 11 491 **5.d. Pegmatites**

12
13
14 492 Pegmatites contain large (5–15 mm) euhedral zoned clinopyroxenes (aegirine-augite to
15
16 493 diopside), ranging from colourless at the core to green at the rim (in PPL) and typically
17
18 494 growing inwards from pegmatite vein margins. These phenocrysts are commonly twinned
19
20 495 and have abundant inclusions of magnetite and fine apatite, particularly concentrated
21
22 496 towards crystal rims. Additionally, finer subhedral clinopyroxene (0.25-1 mm) occurs as a
23
24 497 selvage, commonly clustered around apatite. Acicular or bladed coarse apatite crystals grow
25
26 498 orthogonal to vein margins and also occur as inclusions within clinopyroxene phenocrysts.
27
28 499 They frequently have thin rims of allanite and allanite as fracture infill. Fractures through
29
30 500 pyroxene phenocrysts are infilled by fine K-feldspar or allanite.
31
32
33
34
35

36 501 Feldspars are predominantly coarse K-feldspar, typically with perthitic exsolution with rare
37
38 502 inclusions of magnetite or clinopyroxene (< 0.1 mm). Titanite is common, often clustered
39
40 503 amongst the finer marginal clinopyroxene phases, and is generally subhedral to prismatic.
41
42

43 44 504 **5.e. Allanite veinlets**

45
46
47 505 Allanite is observed as a veining phase within syenite samples (usually restricted to syenites
48
49 506 within the Mixed Syenite Zone, particularly near the hydrothermal biotite-magnetite veins
50
51 507 of the Allt Liath stream section). Such fracture infills (Fig. 9b) are interpreted as evidence for
52
53 508 a period of volatile-rich magmatic-hydrothermal allanite growth, which occurred late in the
54
55 509 history of the intrusion and after crystallisation of host syenites, perhaps due to fluids
56
57
58
59
60

1
2
3 510 introduced to the intrusion during pegmatite crystallisation. It is likely that this stage
4
5 511 resulted from remobilisation of accessory minerals and allanite of primary magmatic origin
6
7 512 within syenites. Brown-orange allanite veinlets vary from < 1 mm to 4 mm thick, cross-cut
8
9 513 and offset by microgranite veins, indicating that this granitic veining stage occurred after
10
11 514 allanite veins. Overall multiple episodes of late fluid-related veinlets of allanite have formed
12
13 515 within the Cnoc nan Cuilean intrusion.
14
15

16
17
18 516 *(Insert Figure 9)*
19
20

21 517 **6. Biotite-magnetite REE-rich veins and metasomatised melasyenites**

22
23
24 518 Material from the biotite-magnetite veins of the Allt Liath stream section in the MZ (as
25
26 519 mentioned in 3.e.) is extremely heterogeneous. In outcrop, moderately altered melasyenitic
27
28 520 wall rock ('biotite-rich inclusions') is observed within the leucosyenites and microgranite
29
30 521 outside of these vein boundaries. Melasyenites included within the biotite-magnetite veins
31
32 522 themselves are completely metasomatised and nodules of this material are suspended in a
33
34 523 highly friable matrix of coarse biotite and magnetite.
35
36
37
38

39 524 **6.a. Biotite-magnetite vein mineralogy**

40
41
42 525 Biotite-magnetite veins are chiefly composed of biotite, magnetite, clinopyroxene, allanite,
43
44 526 apatite, baryte, amphibole, and rare perthitic K-feldspar. In addition a large array of
45
46 527 accessory minerals are also observed, including an allanite-like mineral (a lighter yellow-
47
48 528 brown colour in thin section forming repetitively zoned rims around true allanite crystal
49
50 529 cores – Fig. 10a), strontianite, thorite, and U-Th and U oxides. Various REE- and REE-Sr-
51
52 530 carbonates have also been found as minor veinlets through allanite, the allanite-like
53
54 531 mineral, and apatite in this lithology (Fig. 10a).
55
56
57
58
59
60

1
2
3 532 Multiple stages of mineral growth are observed in biotite-magnetite vein material. Zoned
4
5 533 green clinopyroxene is widespread, varying from coarse crystals to fine clustered and highly
6
7 534 fractured phases. In some cases, small granular pale green clinopyroxene inclusions occur
8
9 535 within coarse tabular biotite. Biotite is widespread with multiple generations. For example,
10
11 536 small tabular brown biotite crystals (< 0.5 mm long) occur within coarse subhedral dark
12
13 537 green biotite. Biotite also occurs in clustered patches or veins, and as discrete tabular
14
15 538 crystals replacing other originally melasyenite mafic minerals (predominantly pyroxenes)
16
17 539 and is commonly associated with amphibole. Magnetite (comprising up to 20% of the
18
19 540 lithology) occurs in two main forms: as a massive vuggy phase with common inclusions of
20
21 541 biotite, apatite, allanite, and baryte (Fig. 10b); and as smaller crystals typically concentrated
22
23 542 at well-defined margins in contact with primary syenites. K-feldspar is normally found
24
25 543 between clinopyroxene clusters and has typically undergone sericitic alteration, but
26
27 544 perthitic exsolution is still locally evident. Allanite and its alteration products are prevalent,
28
29 545 locally comprising 25% of the lithology. This mineral also occurs in several generations
30
31 546 ranging from coarse or blocky core crystals, to highly zoned and complex allanite and
32
33 547 allanite-like mineral layers on crystal rims and infilling fractures. Apatite occurs as massive
34
35 548 rounded clusters of coarse and highly fractured crystals (often with allanite and other rare
36
37 549 earth element (REE)-bearing minerals infilling cracks).

38
39 550 External to the biotite-magnetite veins, moderately altered melasyenite blocks (usually
40
41 551 polygonal) are hosted within leucosyenite or surrounded by microgranite. These still display
42
43 552 relict syenite mineralogy and textures, but carbonate and clays have pervasively and
44
45 553 completely replaced the feldspar component (Fig. 10c). Tabular biotite occurs throughout
46
47 554 (up to c. 50% biotite) locally becoming coarse-grained in proximity to microgranite veinlets
48
49
50
51
52
53
54
55
56
57
58
59
60

1
2
3 555 which cross-cut these altered blocks. Rounded apatite crystals appear unaltered and occur
4
5 556 in carbonate alteration patches and amongst biotite. Apatite commonly has allanite at its
6
7 557 margins, although some coarser examples of allanite (interstitial to apatite and biotite) are
8
9
10 558 also present. Rare relict amphibole and pyroxene are now poikilitic (Fig. 10c) and display
11
12 559 partial overprinting by fine tabular biotite. Unlike material from within the biotite-magnetite
13
14 560 veins however, these metasomatised melasyenites do not display such a wide variety of
15
16 561 accessory minerals (no baryte, strontianite, thorite, U-Th oxides, or REE carbonates have
17
18 562 been observed) and nor do they contain any significant magnetite. In addition, the main
19
20 563 minerals within the biotite-magnetite veins tend to be coarsely crystalline, while these
21
22 564 partially metasomatised rocks external to the veins are generally finer grained.
23
24
25
26

27 565 *(Insert Figure 10)*
28
29

30 566 **6.b. Melasyenite alteration and veining by late fluids**

31
32

33 567 Overall, the textures seen within and around these veins provide evidence of widespread
34
35 568 and variable fluid alteration of the original melasyenites present in this area. Original
36
37 569 primary magmatic mafic minerals have been largely replaced by secondary biotite and the
38
39 570 growth of allanite and magnetite, while feldspars have either been sericitised, kaolinised, or
40
41 571 replaced by carbonates. The high proportion of replacement minerals (biotite \pm magnetite \pm
42
43 572 allanite \pm carbonate \pm clays > 80%) indicates significant metasomatism of melasyenites. The
44
45 573 fluids causing this alteration could have been late-magmatic or hydrothermal in origin. The
46
47 574 variation observed between altered melasyenites within, and external to, biotite-magnetite
48
49 575 veins is likely the result of lesser fluid-present alteration in syenites external to the main
50
51 576 fluid pathway (now inferred by the friable veins themselves), such that the original lithology
52
53 577 is still recognisable in some places. This interpretation is further supported by the frequent
54
55
56
57
58
59
60

1
2
3 578 occurrence (within 30m of biotite-magnetite veins) of leucosyenites and hybrid or mixed
4
5 579 leucosyenite-melasyenites, whose feldspars have undergone extensive sericitisation and
6
7
8 580 kaolinisation, carbonate replacement, and partial replacement of pyroxenes by magnetite. It
9
10 581 may be that further biotite-magnetite veins are present within this area, and that the
11
12 582 structural features of this 'alteration zone' are not fully displayed by the limited and
13
14
15 583 unidirectional exposures of the Allt Liath stream section.
16

17 18 584 **7. Discussion**

19
20
21 585 The Cnoc nan Cuilean intrusion is the smallest (c. 3 km²) and most heterogeneous body
22
23 586 within the Loch Loyal Syenite Complex (Robertson & Parsons, 1974; Parsons, 1999;
24
25 587 Holdsworth *et al.*, 2001), containing multiple igneous lithologies and zones of alteration. We
26
27
28 588 have divided the intrusion into two main zones as described above: the Mixed Syenite Zone
29
30 589 (MZ) and the Massive Leucosyenite Zone (LZ). The field mapping, derived cross-sections, and
31
32
33 590 3D modelling (Fig. 7) indicate that the structure of the Cnoc nan Cuilean intrusion was
34
35 591 initially that of a saucer-shaped lopolith. The first intrusive episode involved passive and
36
37 592 largely concordant emplacement of earlier melasyenitic magmas into a broad plunging
38
39 593 synform within Lewisianoid and Moine rocks. This structural interpretation differs from
40
41
42 594 previously proposed models of a simple NW-trending set of steeply-dipping sheets through
43
44 595 country rock (Holdsworth *et al.*, 1999). Our models clearly show that the main structure
45
46 596 within the intrusion is the gradational contact between the MZ and LZ which extends across
47
48 597 the whole pluton, and is not compatible with emplacement as a series of coalescing sheets.
49
50 598 Sheeted contacts are evident in some of the northern marginal areas of the intrusion (for
51
52 599 the LZ in the NW margin, and MZ and LZ in the NE margin) where sheeting and minor
53
54
55 600 veining of melts occurs and is most typically concordant with the gently-dipping fabric in the
56
57
58
59
60

1
2
3 601 country rock. Xenoliths were incorporated as magma fingered out into the surrounding host
4
5 602 rock from a feeder zone, thought to be situated towards the western side of the intrusion,
6
7 603 just south of Cnoc nan Cuilean itself. During a second intrusive episode, felsic syenitic
8
9 604 magmas were emplaced, intruding into and mixing with the earlier melasyenite lopolith to
10
11 605 ultimately form the MZ. Textural evidence suggests that the melasyenites of the MZ were a
12
13 606 crystal mush of variable melt fractions, hence producing a variation from lobate blebs of the
14
15 607 mingled syenitic magmas, to gradational changes from one syenite lithology to another,
16
17 608 suggesting a chemical as well as a physical interaction and assimilation during mixing. This
18
19 609 would therefore imply no major break in the magmatic replenishment of the Cnoc nan
20
21 610 Cuilean intrusion (between Stages 1 and 2, Fig. 11). During this episode country rock
22
23 611 xenoliths within the melasyenites were fractured and veined by leucosyenite, and additional
24
25 612 new country rock xenoliths became entrained.
26
27
28
29
30
31

32 613 Continuing leucosyenite intrusion into higher levels of the lopolith eventually led to the
33
34 614 formation of the LZ (Stage 2 – Fig. 11) with magma being fed along two main faults (trending
35
36 615 approximately N–S and NE–SW) resulting in the observed elongate structure of the LZ
37
38 616 forming the high ground of Creag nan Cat. In areas closer to the inferred feeder zone,
39
40 617 homogeneous LZ syenites were formed as the intrusion inflated from the centre of the
41
42 618 leucosyenite intrusion, such that early mafic material became inundated or fully assimilated,
43
44 619 leaving little evidence of the early melasyenites in these western, central, and higher areas
45
46 620 of the intrusion. However this was a variable process, and hence the boundary between
47
48 621 what is now the MZ and LZ is a gradual one. Evidence of emplacement of two (or more)
49
50 622 magma batches distinguishes the Cnoc nan Cuilean intrusion from the other more
51
52 623 homogeneous intrusions within the Loch Loyal Syenite Complex (Parsons, 1999) and
53
54
55
56
57
58
59
60

1
2
3 624 suggests a prolonged magmatic history involving multiple episodes of magma
4
5 625 replenishment.
6
7

8
9 626 Overall, the entire intrusion process was likely initially facilitated by late Caledonian gravity-
10
11 627 driven extension of Moine Thrust sheets (Holdsworth *et al.*, 1999). Melt ingress was aided
12
13 628 by extensional faulting observed across the pluton, particularly in an E-W direction (Stage 1
14
15 629 – Fig. 11). All magmatic units were fed from a deeper evolving and replenishing magma
16
17 630 chamber up to the lopolith level. This mechanism has been inferred for the Ben Loyal
18
19 631 intrusion, with the foliations observed in its marginal zones thought to have developed
20
21 632 during the movement of a nearly solid crystal mush (Robertson & Parsons, 1974). This
22
23 633 supports the hypothesis of mobile partially crystalline melts moving to higher crustal
24
25 634 regions.
26
27
28
29

30
31 635 Throughout magma batch replenishment, the variable volatile content led to patchy and
32
33 636 variable forms of pegmatite veining, allanite stringers, or a combination of the two occurring
34
35 637 as long narrow veins and irregular inclusions within syenites, often cross-cut and offset by
36
37 638 later microgranite veins. These microgranite veins post-date all other lithologies within the
38
39 639 Cnoc nan Cuilean intrusion and thus represent the last magmatic event.
40
41
42

43
44 640 In the waning stages of magmatism, an episode of fluid-present alteration led to the
45
46 641 crystallisation of coarse biotite, magnetite, hornblende, and allanite in discrete sub-vertical
47
48 642 veins within the MZ. The Allt Liath stream section displays three N-S trending, steeply
49
50 643 dipping narrow veins of this type. The fluids responsible for the alteration may be late-
51
52 644 magmatic metasomatic, or may be derived from a hydrothermal system. In some cases, a
53
54 645 fine anastomosing network of microgranite veinlets can be observed within these zones. It is
55
56 646 therefore suggested that the modifying fluid phase and the invasive microgranite veining
57
58
59
60

1
2
3 647 lithology are broadly coeval (Stage 3 – Fig. 11), perhaps with the replenishing batch of
4
5 648 magma ultimately introducing a large volume of metasomatic fluids, resulting in fluid-rich
6
7 649 alteration. Thus, given the extensive occurrences of microgranitic veins, it is possible that
8
9 650 biotite-magnetite veins may be more extensive in the MZ than currently suggested by
10
11 651 surface exposure. However due to their friable nature and vulnerability to erosion, these are
12
13 652 not exposed on the highly vegetated and peat-covered surfaces of the intrusion.
14
15
16

17
18 653 During biotite-magnetite vein formation in the MZ, host syenites were variably
19
20 654 metasomatically altered. During this process, syenites underwent almost complete
21
22 655 replacement of the primary magmatic mineralogy by coarse biotite, magnetite,
23
24 656 clinopyroxene, allanite, apatite, and carbonates. These highly altered biotite-magnetite
25
26 657 lithologies are most commonly found within the north-south veins, but also occur in discrete
27
28 658 patches in the surrounding MZ syenites of Allt Liath, often associated with microgranite.
29
30 659 This may indicate the presence of more biotite-magnetite veins in this area, since eroded or
31
32 660 forming a more complex 3D arrangement.
33
34
35
36

37
38 661 The apparent scarcity of these biotite-magnetite veins may be due to their weathering
39
40 662 propensity and extreme friability, and thus it is likely that these have been preferentially
41
42 663 eroded. We consider it likely that a much more extensive network of these veins exists,
43
44 664 however these will only be identifiable by geophysical studies due to the lack of exposure.
45
46 665 Overall the structural control on this alteration event remains unclear. The biotite-
47
48 666 magnetite vein occurrence at the intrusion margin may have resulted from the potentially
49
50 667 greater mobility of fluids in this region with veins trending parallel to the intrusion edge.
51
52 668 Alternatively the veins could be infilling a N-S-trending fracture system.
53
54
55
56
57
58
59
60

1
2
3 669 The Loch Loyal Syenite Complex is enriched in the rare earth elements (REE) relative to
4
5 670 other intrusions in the UK, even in the more homogeneous syenites of its three constituent
6
7 671 intrusions (Plant *et al.*, 1969; Shaw & Gunn, 1993). It represents an enriched member of the
8
9
10 672 Caledonian Parental Magma Array (Halliday *et al.*, 1987; Fowler *et al.*, 2008). At Cnoc nan
11
12 673 Cuilean, REE-bearing minerals (predominantly LREE-rich allanite) are concentrated in the
13
14 674 melasyenites of the MZ, and particularly in the altered biotite-magnetite veins. The REE are
15
16 675 incompatible, and so REE-bearing minerals might generally be expected to be found in
17
18 676 more-evolved magmatic lithologies, such as pegmatites. However, at Cnoc nan Cuilean, the
19
20 677 REE are concentrated in accessory minerals (particularly allanite) which are most abundant
21
22 678 in the more mafic, less-evolved lithologies (melasyenites) and are then further concentrated
23
24 679 through alteration by late-stage fluids of magmatic or hydrothermal origin. The MZ is not
25
26 680 well exposed, and may potentially contain more areas of alteration that have similarly high
27
28 681 REE contents. It is likely that similar processes operate in other intrusions, and therefore this
29
30 682 has important consequences for our understanding of how REE-bearing minerals form, and
31
32 683 hence for REE exploration.
33
34
35
36
37
38

39 684 This work has allowed us to develop a clearer picture of the structure of the Cnoc nan
40
41 685 Cuilean intrusion, aiding future exploration for REE mineralisation in this and other similarly
42
43 686 poorly exposed intrusive bodies. Key to this success has been the development of a working
44
45 687 and interactive 3D model, constructed from field mapping data equivalent to that obtained
46
47 688 during early-stage mineral reconnaissance and exploration programmes. The intrusion may
48
49 689 further be used to understand the processes by which REE become concentrated in
50
51 690 magmatic and post-magmatic settings.
52
53
54

55
56 691 *(Insert Figure 11)*
57
58
59
60

1
2
3 692 **8. Conclusions**
4
5

6 693 New mapping presented here contributes to a new interpretation of the structure of the
7
8 694 intrusion, demonstrating that an initially lopolith shaped melasyenite magma body was
9
10 695 inundated by leucosyenites during its crystallisation. Thus the intrusion can be divided into
11
12 696 two zones according to melasyenite content, with a gradational boundary in between them.
13
14 697 In addition, pegmatites, allanite- and pyroxene stringers, and microgranite veins are
15
16 698 widespread throughout the intrusion. LREE-bearing minerals, predominantly allanite, are
17
18 699 concentrated in melasyenites rather than in the more evolved leucosyenites. In turn,
19
20 700 allanite has been further concentrated in biotite- and magnetite-rich veins on the eastern
21
22 701 side of the intrusion by late fluid alteration. This has significantly enriched REE in these
23
24 702 structures.
25
26
27
28
29

30 703 Together with cross-sections, mapping has been used to build an interactive 3D GoCAD™
31
32 704 model of the Cnoc nan Cuilean syenite body. The model has allowed for the testing of
33
34 705 structural interpretations and cross-section validity relative to known field observations.
35
36 706 This provides a low cost working visualisation process that can be employed at a very early
37
38 707 stage in exploration or mineral reconnaissance in complex igneous geology settings
39
40 708 suffering from limited exposure. With the novel and innovative use of a 3D intrusion model,
41
42 709 a more detailed understanding of the intrusion's shape and thus the areas of potential
43
44 710 interest for REE mineralisation can be established. Overall this intrusion contributes to our
45
46 711 understanding of processes important to critical metal metallogenesis.
47
48
49
50
51

52 712
53
54
55
56
57
58
59
60

1
2
3 713 *Acknowledgements*
4

5 714 *The authors would like to thank colleagues at BGS (Keyworth and Edinburgh) for help and discussion during this*
6

7 715 *research. M. Fowler (University of Portsmouth) and an anonymous reviewer are thanked for their helpful*
8

9 716 *comments towards the manuscript. Thanks are extended to M. Styles, T. Milodowski, J. Rushton and M. Allen*
10

11 717 *(Keyworth). C. Richie, T. Kearsey and R. Terrington are thanked for their part in the production of the 3D model.*
12

13 718 *Lastly, J. Hughes and D. Paterson are thanked for their logistical aid in the field, along with the staff and*
14

15 719 *proprietors of the Tongue Hotel for such a pleasant stay during fieldwork. H.S.R.H. acknowledges the financial*
16

17 720 *support of the Natural Environment Research Council (NERC); the BGS University Funding Initiative (BUFI); and*
18

19 721 *the Schools Competition Act Settlement Trust (SCAST) for sponsorship of this research.*
20

21
22 722
23
24
25
26
27
28
29
30
31
32
33
34
35
36
37
38
39
40
41
42
43
44
45
46
47
48
49
50
51
52
53
54
55
56
57
58
59
60

723

724

References:

725

726 ATHERTON, M. P. & GHANI, A. A. 2002. Slab breakoff: a model for Caledonian, late granite syn-
727 collisional magmatism in the orthotectonic (metamorphic) zone of Scotland and Donegal,
728 Ireland. *Lithos*, **62**, 65-85.

729 COWARD, M. P. 1990. The Precambrian, Caledonian and Variscan framework to NW Europe.
730 *Geological Society, London, Special Publications*, **55**, 1-34.

731 DEWEY, J. F. & STRACHAN, R. A. 2003. Changing Silurian-Devonian relative plate motion in the
732 Caledonides: sinistral transpression to sinistral transtension. *Journal of the Geological Society*,
733 *London*, **160**, 219-229.

734 FOWLER, M. B. 1988. Elemental evidence for crustal contamination of mantle-derived Caledonian
735 syenite by metasediment anatexis and magma mixing. *Chemical Geology*, **69**, 1-16.

736 FOWLER, M. B. 1992. Elemental and O-Sr-Nd isotope geochemistry of the Glen Dessarry syenite, NW
737 Scotland. *Journal of the Geological Society*, **149**, 209-220.

738 FOWLER, M. B. & HENNEY, P. J. 1996. Mixed Caledonian appinite magmas: Implications for
739 lamprophyre fractionation and high Ba-Sr granite genesis. *Contributions to Mineralogy and*
740 *Petrology*, **126**, 199-215.

741 FOWLER, M. B., HENNEY, P. J., DARBYSHIRE, D. P. F. & GREENWOOD, P. B. 2001. Petrogenesis of high Ba-Sr
742 granites: the Rogart pluton, Sutherland. *Journal of the Geological Society, London*, **158**, 521-
743 534.

744 FOWLER, M. B., KOCKS, H., DARBYSHIRE, D. P. F. & GREENWOOD, P. B. 2008. Petrogenesis of high Ba-Sr
745 plutons from the Northern Highlands Terrane of the British Caledonian Province. *Lithos*, **105**,
746 129-148.

747 GALLAGHER, M. J., MICHIE, U. M., SMITH, R. T. & HAYNES, L. 1971. New evidence of uranium and other
748 mineralization in Scotland. *Transactions of the Institution of Mining and Metallurgy*, **80**, 150-
749 173.

750 GALLON, A. C. 1974. *Geological and geochemical aspects of the Loch Loyal Alkaline Complex*,
751 *Sutherland*. PhD, University of Leeds.

752 GOODENOUGH, K. M., MILLAR, I., STRACHAN, R. A., KRABBENDAM, M., *et al.* 2011. Timing of regional
753 deformation and development of the Moine Thrust Zone in the Scottish Caledonides:
754 constraints from the U-Pb geochronology of alkaline intrusions. *Journal of the Geological*
755 *Society, London*, **168**, 99-114.

756 GOODENOUGH, K. M., YOUNG, B. N. & PARSONS, I. 2004. The minor intrusions of Assynt, NW Scotland:
757 early development of magmatism along the Caledonian Front. *Mineralogical Magazine*, **68**,
758 541-559.

759 HALLIDAY, A. N., AFTALION, M., PARSONS, I., DICKIN, A. P., *et al.* 1987. Syn-orogenic alkaline magmatism
760 and its relationship to the Moine Thrust Zone and the thermal state of the Lithosphere in
761 NW Scotland. *Journal of the Geological Society, London*, **144**, 611-617.

762 HOLDSWORTH, R. E., McERLEAN, M. A. & STRACHAN, R. A. 1999. The influence of country rock structural
763 architecture during pluton emplacement: the Loch Loyal syenites, Scotland. *Journal of the*
764 *Geological Society, London*, **156**, 163-175.

765 HOLDSWORTH, R. E., STRACHAN, R. A. & ALSOP, G. I. 2001. *Solid geology of the Tongue District: Memoir*
766 *for 1:50,000 Geological Sheet 114E (Scotland)*, British Geological Survey.

767 JOHNSTONE, G. S. & MYKURA, W. 1989. Younger Caledonian igneous rocks. *In: British Regional Geology:*
768 *The Northern Highlands of Scotland*. pp. 102-117. British Geological Survey. 4th ed.

769 KING, B. C. 1942. The Cnoc nan Cuilean area of the Ben Loyal Igneous Complex. *Quarterly Journal of*
770 *the Geological Society*, **98**, 147-185.

771 MALLET, J. L. 1997. Discrete Modeling for Natural Objects. *Mathematical Geology*, **29**, 199-219.

772 MALLET, J. L. 2002. *Geomodeling*, New York, Oxford University Press.

1
2
3
4
5
6
7
8
9
10
11
12
13
14
15
16
17
18
19
20
21
22
23
24
25
26
27
28
29
30
31
32
33
34
35
36
37
38
39
40
41
42
43
44
45
46
47
48
49
50
51
52
53
54
55
56
57
58
59
60

- 1
2
3 773 MCERLEAN, M. A., HOLDSWORTH, R. E. & STRACHAN, R. A. 1992. The deformation and emplacement of
4 774 the Loch Loyal Syenite Complex, Northern Scotland. *Joint Annual Meeting of the*
5 775 *Mineralogical Society of Canada and the Geological Association of Canada*. Acadia
6 776 University, Wolfvill, Nova Scotia: Geological Association of Canada.
7 777 MCKERROW, W. S., MACNIOCAILL, C. & DEWEY, J. F. 2000. The Caledonian Orogeny redefined. *Journal of*
8 778 *the Geological Society, London*, **157**, 1149-1154.
9 779 MOORHOUSE, S. J. & MOORHOUSE, V. E. 1977. A Lewisian basement sheet within the Moine at Ribigill,
10 780 north Sutherland. *Scottish Journal of Geology*, **13**, 289-300.
11 781 PARSONS, I. 1968. The origin of the basic and ultrabasic rocks of the Loch Ailsh alkaline intrusion,
12 782 Assynt. *Scottish Journal of Geology*, **4**, 221-234.
13 783 PARSONS, I. 1972. Comparative petrology of the leucocratic syenites of the Northwest Highlands of
14 784 Scotland. *Geological Journal*, **8**, 71-82.
15 785 PARSONS, I. 1999. Loch Loyal Syenite Complex. *In: Caledonian Igneous Rocks of Great Britain*. (eds.
16 786 STEPHENSON, D., BEVINS, R. E., MILLWARD, D., HIGHTON, A. J., *et al.*).
17 787 PLANT, J. A., GALLAGHER, M. J. & SMITH, R. T. 1969. Geochemical survey of the Ben Loyal syenite
18 788 complex, Sutherland. London: Institute of Geological Sciences, Radiogeology and Rare
19 789 Minerals Unit.
20 790 READ, H. H. 1931. *The geology of central Sutherland*.
21 791 ROBERTSON, R. C. R. & PARSONS, I. 1974. The Loch Loyal Syenites. *Scottish Journal of Geology*, **10**, 129-
22 792 146.
23 793 SHAW, M. H. & GUNN, A. G. 1993. Rare Earth Elements in Alkaline Intrusions North-West Scotland.
24 794 *Mineral Reconnaissance Programme*. British Geological Survey.
25 795 SOPER, N. J., STRACHAN, R. A., HOLDSWORTH, R. E., GAYER, R. A., *et al.* 1992. Sinistral transpression and
26 796 the Silurian closure of Iapetus. *Journal of the Geological Society, London*, **149**, 871-880.
27 797 TANNER, P. W. G. 1970. The Sgurr Beag Slide—a major tectonic break within the Moinian of the
28 798 Western Highlands of Scotland. *Quarterly Journal of the Geological Society*, **126**, 435-463.
29 799 TARNEY, J. & JONES, C. E. 1994. Trace element geochemistry of orogenic igneous rocks and crustal
30 800 growth models. *Journal of the Geological Society, London*, **151**, 855-868.
31 801 THOMPSON, R. N. & FOWLER, M. B. 1986. Subduction-related shoshonitic and ultrapotassic magmatism:
32 802 a study of Siluro-Ordovician syenites from the Scottish Caledonides. *Contributions to*
33 803 *Mineralogy and Petrology*, **94**, 507-522.
34 804 TORSVIK, T. H., SMETHURST, M. A., MEERT, J. G., VAN DER VOO, R., *et al.* 1996. Continental break-up and
35 805 collision in the Neoproterozoic and Palaeozoic - A tale of Baltica and Laurentia. *Earth-Science*
36 806 *Reviews*, **40**, 229-258.
37 807
38 808
39
40
41
42 809
43
44
45
46
47
48
49
50
51
52
53
54
55
56
57
58
59
60

1
2
3 810 **List of figure captions:**
4
5

6 811 *Figure 1.* Simplified regional geological map of NW Scotland, displaying the main faults,
7
8 812 thrust, and Caledonian intrusions. Major thrusts include: Moine Thrust (MT), Naver Thrust
9
10 813 (NT), Ben Hope Thrust (BHT), and the Sgurr Beag Thrust (SBT). Location of Figure 2 indicated
11
12 814 in boxed area. Figure adapted from Goodenough *et al.* (2011). British National Grid
13
14 815 coordinates (NC) provided.
15
16
17

18 816 *Figure 2.* Geology of the Loch Loyal Syenite Complex based on King (1942), Robertson and
19
20 817 Parsons (1974), Holdsworth *et al.* (1999), Holdsworth *et al.* (2001), published BGS 1:50,000
21
22 818 geological maps of the area, and the new mapping presented here. Three individual
23
24 819 intrusions: Ben Loyal (BL), Beinn Stumanadh (BS), and Cnoc nan Cuilean (CnC). Faults
25
26 820 including the Loch Loyal Fault and two faults (F1 and F2) within the Cnoc nan Cuilean
27
28 821 intrusion. Surrounding country rock foliations delineated from field measurements and
29
30 822 adapted from Holdsworth *et al.* 1999. Location of Figure 3 indicated by boxed area. British
31
32 823 National Grid coordinates (NC) provided.
33
34
35
36
37

38 824 *Figure 3.* Detailed geology of the Cnoc nan Cuilean intrusion. Inset boxes indicate positions
39
40 825 of close-up maps (Fig. 5) around the intrusion margins. Vein size has been over-emphasised
41
42 826 for clarity in figure. Fault 1 (F1) and Fault 2 (F2) displayed. British National Grid coordinates
43
44 827 (NC) provided.
45
46
47

48 828 *Figure 4.* (Colour online) Field and hand sample photographs of mixing/mingling textures
49
50 829 observed throughout the Cnoc nan Cuilean intrusion. (a) Lobate contact of dark-coloured
51
52 830 melasyenites with lighter leucosyenites (contact highlighted by white lines). (b) Examples of
53
54 831 melasyenite-leucosyenite complex mixing and mingling textures (solid lines indicate
55
56
57
58
59
60

1
2
3 832 mingling between melasyenite and leucosyenite, while dashed circles highlight gradational
4
5 833 relationships between these two lithologies, suggesting mixing). (c) Cut hand sample of
6
7
8 834 melasyenite and leucosyenite contact. Note the later leucosyenite vein (Lsy(2)) within Lsy(1)
9
10 835 earlier leucosyenite unit. (d) Pegmatite within leucosyenite (pegmatite contacts shown by
11
12 836 white lines, with pyroxene selvage at margin). (e) Hand sample of nodule from a biotite-
13
14
15 837 magnetite vein (Allt Liath) showing leucosyenite veining, coarse and vuggy magnetite and
16
17 838 dark-coloured mineral phases including clinopyroxene, biotite, and allanite. (f) Leucosyenite
18
19 839 with altered and metasomatised country rock (?Lewisianoid) xenolith displaying relict
20
21 840 foliation. Black lines highlight cross-cutting microgranite veinlets.
22
23

24
25 841 *Figure 5.* Close-up maps of the Cnoc nan Cuilean intrusion margins delineating country rock
26
27 842 foliation, structural measurements, and concordant and discordant veins. British National
28
29 843 Grid coordinates (NC) provided.
30
31

32
33 844 *Figure 6.* Cross-sections of the Cnoc nan Cuilean intrusion showing broad synform within the
34
35 845 country rocks, into which the lopolith form of the MZ sits, overprinted by later intrusive
36
37 846 events associated with the LZ. LLF is Loch Loyal Fault, F1 and F2 are Faults 1 and 2
38
39 847 respectively, within the Cnoc nan Cuilean intrusion.
40
41

42
43 848 *Figure 7.* (colour online) Snapshot views of the 3D GoCAD™ model of the Cnoc nan Cuilean
44
45 849 intrusion. (a) Plan view of the intrusion showing contoured topographic surface. (b) View
46
47 850 from beneath the NW corner of the intrusion. (c) View from E of the intrusion,
48
49 851 demonstrating the lopolith shape of the MZ and more elongate vertical body of the MZ
50
51 852 (white line indicates ground level of the margin of the intrusion). (d) View from N of the
52
53 853 intrusion. MZ is the yellow body (or lighter grey in print), LZ is the red body (or darker grey
54
55 854 in print).
56
57
58
59
60

1
2
3 855 *Figure 8.* (Colour online) Photomicrographs of textures for syenites. (a) Clustered
4
5 856 clinopyroxene, titanite, and apatite in melasyenite stringer. Fine dark brown allanite
6
7 857 interstitial within this stringer. Coarse perthitic K-feldspar either side of mafic mineral
8
9
10 858 stringer. (b) Example orbicular texture in melasyenite, with green clinopyroxene, amphibole,
11
12 859 and titanite forming rounded clusters between coarse K-feldspar crystals. Orbicule centres
13
14 860 also with coarse perthitic K-feldspar. (c) Coarse rounded apatite crystal (from melasyenite)
15
16 861 with a partial allanite rim and surrounded by K-feldspar (with albite exsolution) and
17
18 862 prismatic clinopyroxene. Apatite is inclusion-rich (often magnetite flecks) with allanite
19
20 863 infilling fractures.
21
22
23
24

25 864 *Figure 9.* Selection of Scanning Electron Microscope Back Scattered Electron images of
26
27 865 samples from the Cnoc nan Cuilean intrusion. (a) Interstitial allanite between euhedral and
28
29 866 subhedral clinopyroxene, titanite, and apatite (with K-feldspar and albite exsolution
30
31 867 lamellae in top of view) in melasyenite. (b) Allanite infilling fractures through coarse
32
33 868 clinopyroxene crystals within melasyenite sample. Bright thorite also seen as rounded
34
35 869 crystals infilling vugs or fractures. Mineral abbreviations: apatite (Ap), clinopyroxene (Cpx),
36
37 870 titanite (Ttn), allanite (Aln), and thorite (Thr).
38
39
40
41

42 871 *Figure 10.* Scanning Electron Microscope Back Scattered Electron image of biotite-magnetite
43
44 872 vein material showing (a) allanite with an allanite-like banded mineral and (b) baryte,
45
46 873 thorite, and apatite infilling a large vug within a fractured magnetite crystal. (c)
47
48 874 Photomicrograph of a metasomatised melasyenite sample exposed adjacent and external to
49
50 875 biotite-magnetite veins. Poikilitic amphibole has abundant inclusions of apatite, while small
51
52 876 tabular biotite and cryptocrystalline carbonate replace and overprint the original feldspar
53
54 877 component of the syenite. Mineral abbreviations: apatite (Ap), clinopyroxene (Cpx),
55
56
57
58
59
60

1
2
3 878 amphibole (Am), biotite (Bt), titanite (Ttn), allanite (Aln), allanite-like mineral (Aln-like),
4
5 879 magnetite (Mag), thorite (Thr), baryte (Brt), REE-Sr carbonate veining mineral (REE-Sr carb),
6
7
8 880 and carbonate (CO₃).
9

10
11 881 *Figure 11.* Schematic diagram demonstrating the formation events of the Cnoc nan Cuilean
12
13 882 intrusion.
14

15
16 883
17
18
19
20
21
22
23
24
25
26
27
28
29
30
31
32
33
34
35
36
37
38
39
40
41
42
43
44
45
46
47
48
49
50
51
52
53
54
55
56
57
58
59
60

Proof For Review

1
2
3
4
5
6
7
8
9
10
11
12
13
14
15
16
17
18
19
20
21
22
23
24
25
26
27
28
29
30
31
32
33
34
35
36
37
38
39
40
41
42
43
44
45
46
47
48
49
50
51
52
53
54
55
56
57
58
59
60

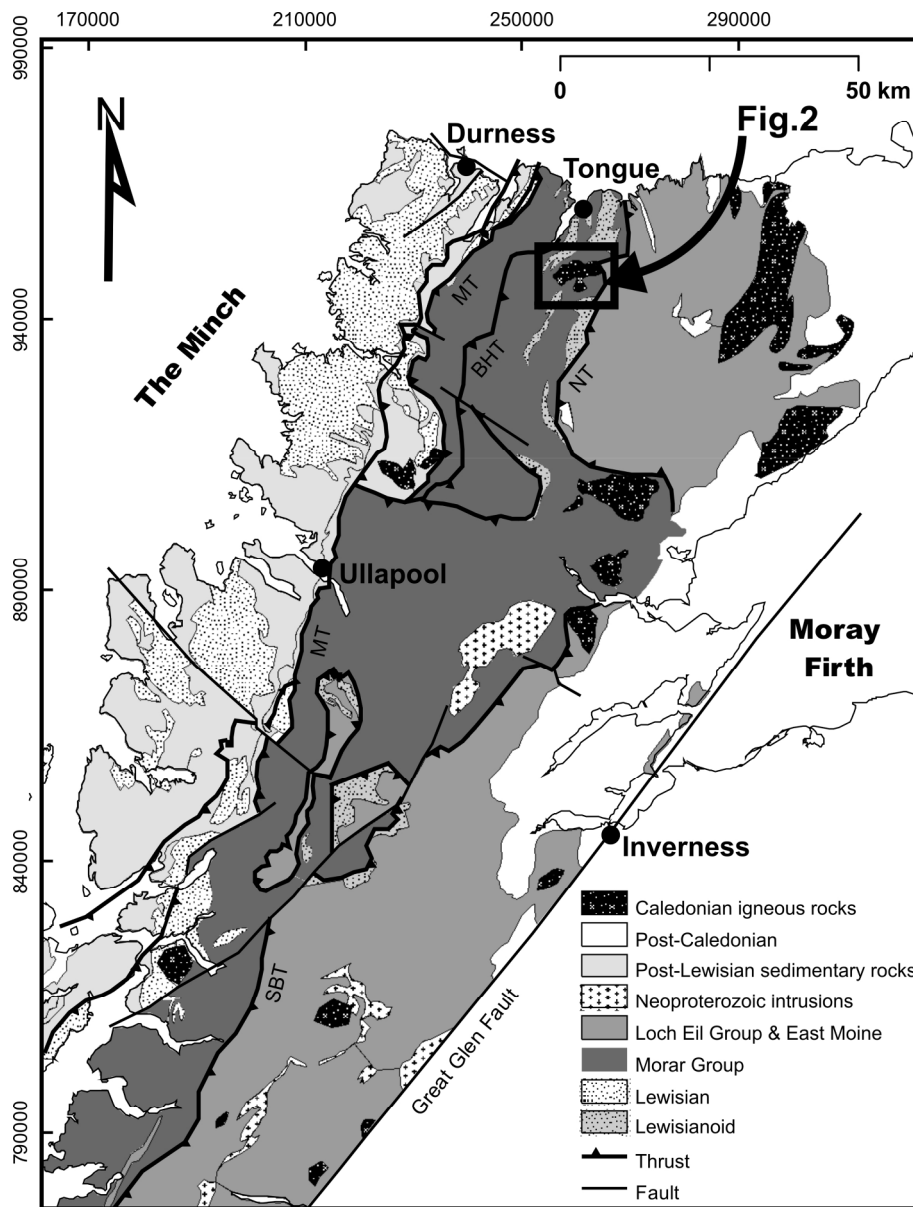


Figure 1. Simplified regional geological map of NW Scotland, displaying the main faults, thrust, and Caledonian intrusions. Major thrusts include: Moine Thrust (MT), Naver Thrust (NT), Ben Hope Thrust (BHT), and the Sgurr Beag Thrust (SBT). Location of Figure 2 indicated in boxed area. Figure adapted from Goodenough et al. (2011). British National Grid coordinates (NC) provided. 99x131mm (600 x 600 DPI)

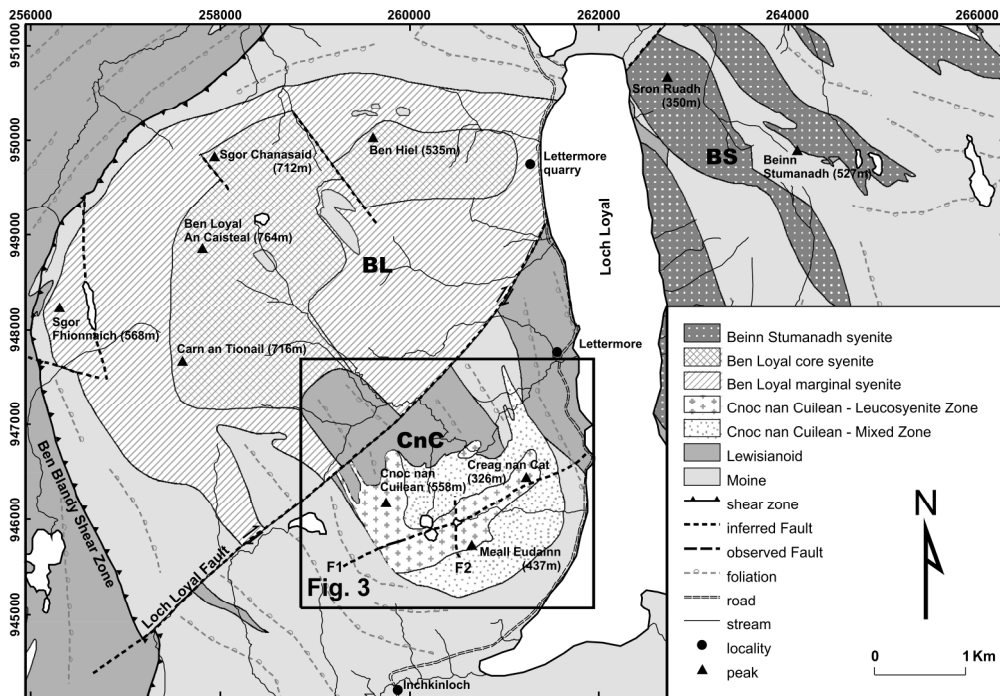


Figure 2. Geology of the Loch Loyal Syenite Complex based on King (1942), Robertson and Parsons (1974), Holdsworth et al. (1999), Holdsworth et al. (2001), published BGS 1:50,000 geological maps of the area, and the new mapping presented here. Three individual intrusions: Ben Loyal (BL), Beinn Loyal (BL), and Cnoc nan Cuilean (CnC). Faults including the Loch Loyal Fault and two faults (F1 and F2) within the Cnoc nan Cuilean intrusion. Surrounding country rock foliations delineated from field measurements and adapted from Holdsworth et al. 1999. Location of Figure 3 indicated by boxed area. British National Grid coordinates (NC) provided.
114x78mm (600 x 600 DPI)

view

1
2
3
4
5
6
7
8
9
10
11
12
13
14
15
16
17
18
19
20
21
22
23
24
25
26
27
28
29
30
31
32
33
34
35
36
37
38
39
40
41
42
43
44
45
46
47
48
49
50
51
52
53
54
55
56
57
58
59
60

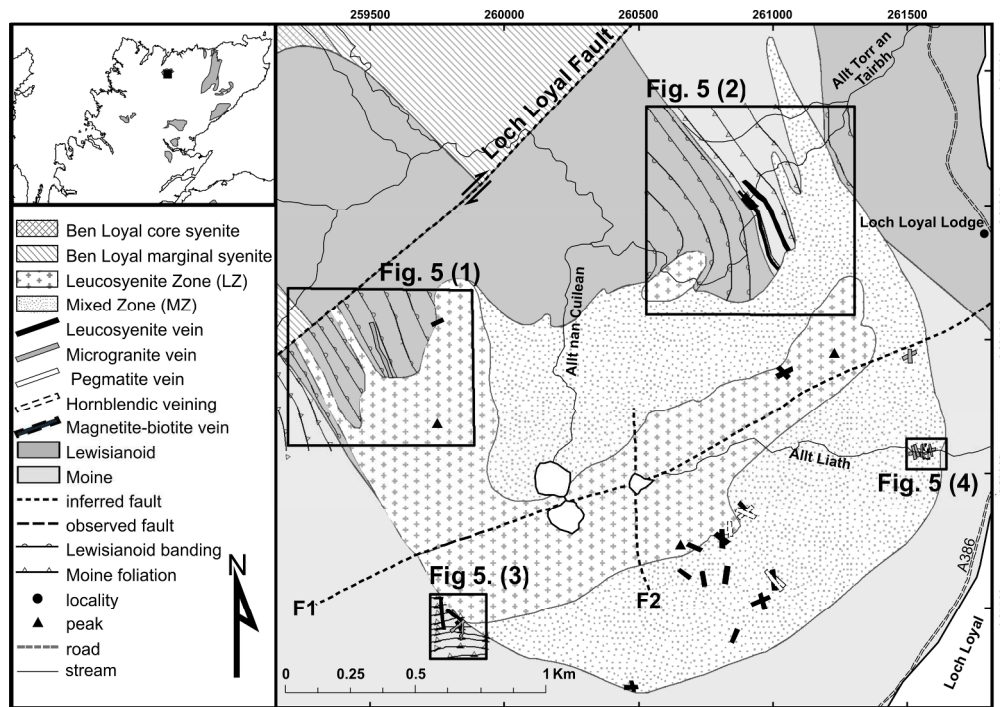


Figure 3. Detailed geology of the Cnoc nan Cuilean intrusion. Inset boxes indicate positions of close-up maps (Fig. 5) around the intrusion margins. Vein size has been over-emphasised for clarity in figure. Fault 1 (F1) and Fault 2 (F2) displayed. British National Grid coordinates (NC) provided.
117x81mm (600 x 600 DPI)

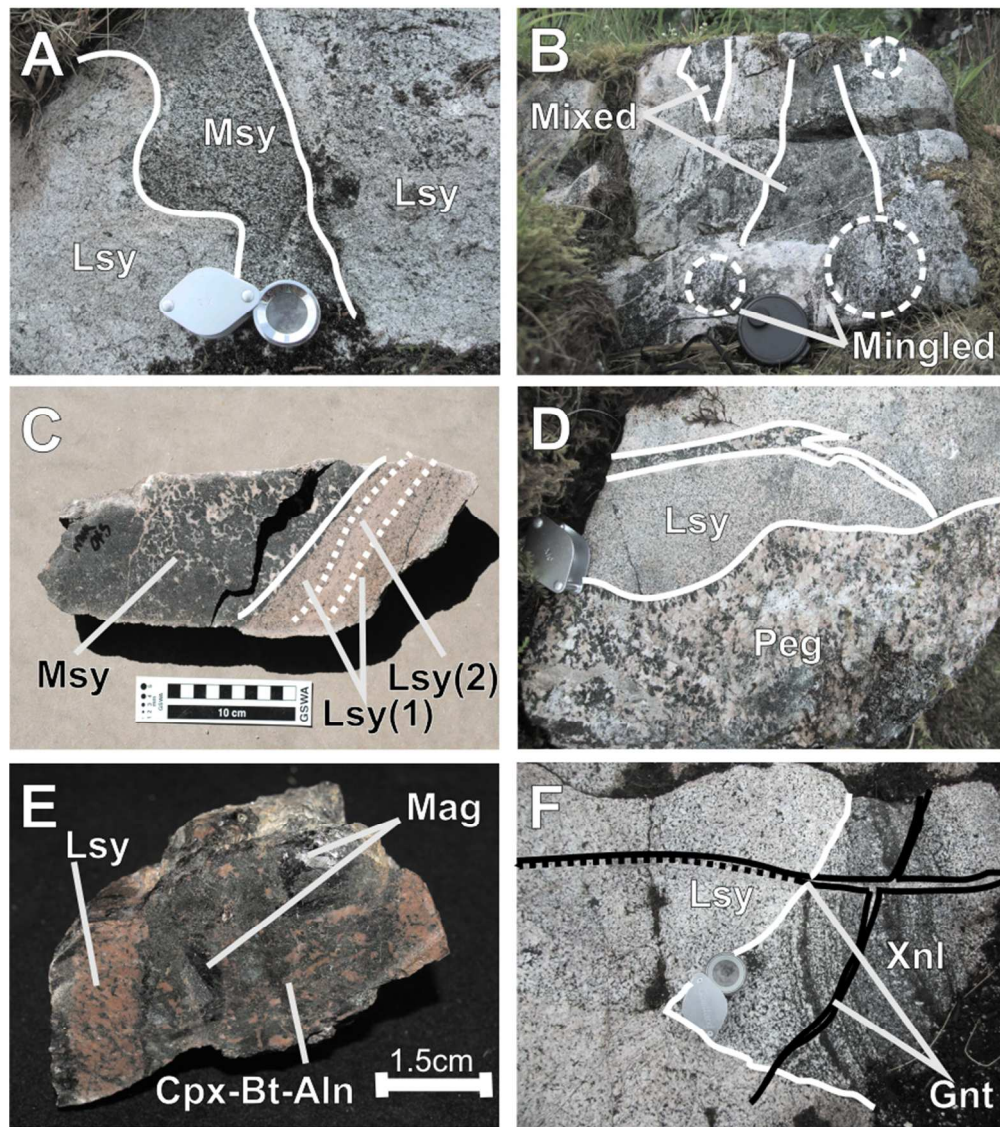


Figure 4. (Colour online) Field and hand sample photographs of mixing/mingling textures observed throughout the Cnoc nan Cuilean intrusion. (a) Lobate contact of dark-coloured melasyenites with lighter leucosyenites (contact highlighted by white lines). (b) Examples of melasyenite-leucosyenite complex mixing and mingling textures (solid lines indicate mingling between melasyenite and leucosyenite, while dashed circles highlight gradational relationships between these two lithologies, suggesting mixing). (c) Cut hand sample of melasyenite and leucosyenite contact. Note the later leucosyenite vein (Lsy(2)) within Lsy(1) earlier leucosyenite unit. (d) Pegmatite within leucosyenite (pegmatite contacts shown by white lines, with pyroxene selvage at margin). (e) Hand sample of nodule from a biotite-magnetite vein (Allt Liath) showing leucosyenite veining, coarse and vuggy magnetite and dark-coloured mineral phases including clinopyroxene, biotite, and allanite. (f) Leucosyenite with altered and metasomatised country rock (?Lewisianoid) xenolith displaying relict foliation. Black lines highlight cross-cutting microgranite veinlets. 78x88mm (300 x 300 DPI)

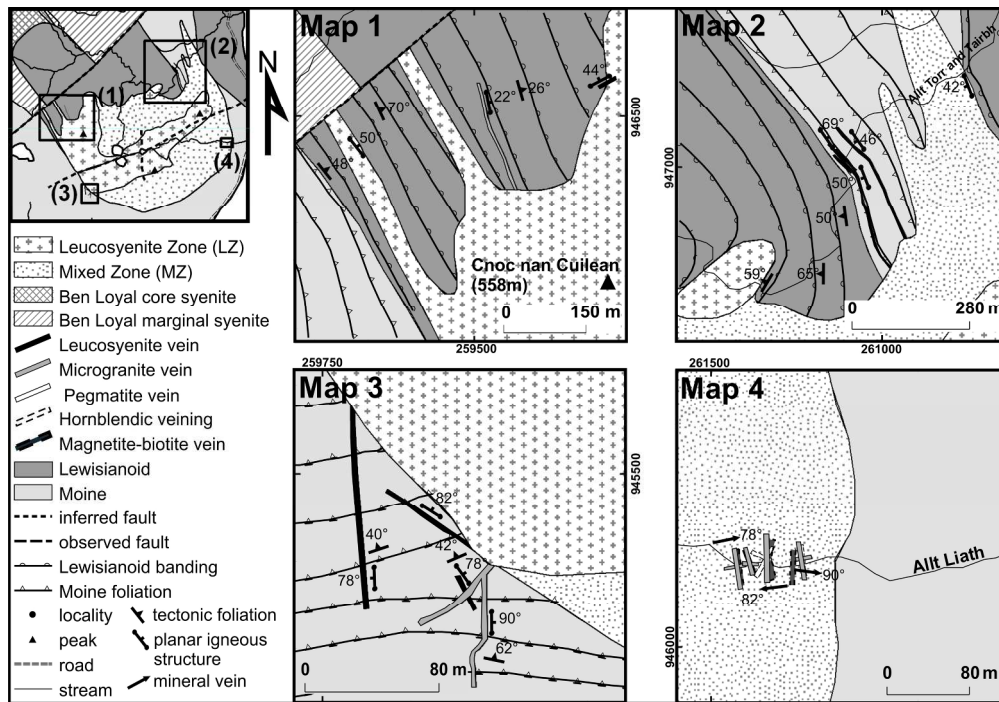


Figure 5. Close-up maps of the Cnoc nan Cuilean intrusion margins delineating country rock foliation, structural measurements, and concordant and discordant veins. British National Grid coordinates (NC) provided.
 116x80mm (600 x 600 DPI)

Review

1
2
3
4
5
6
7
8
9
10
11
12
13
14
15
16
17
18
19
20
21
22
23
24
25
26
27
28
29
30
31
32
33
34
35
36
37
38
39
40
41
42
43
44
45
46
47
48
49
50
51
52
53
54
55
56
57
58
59
60

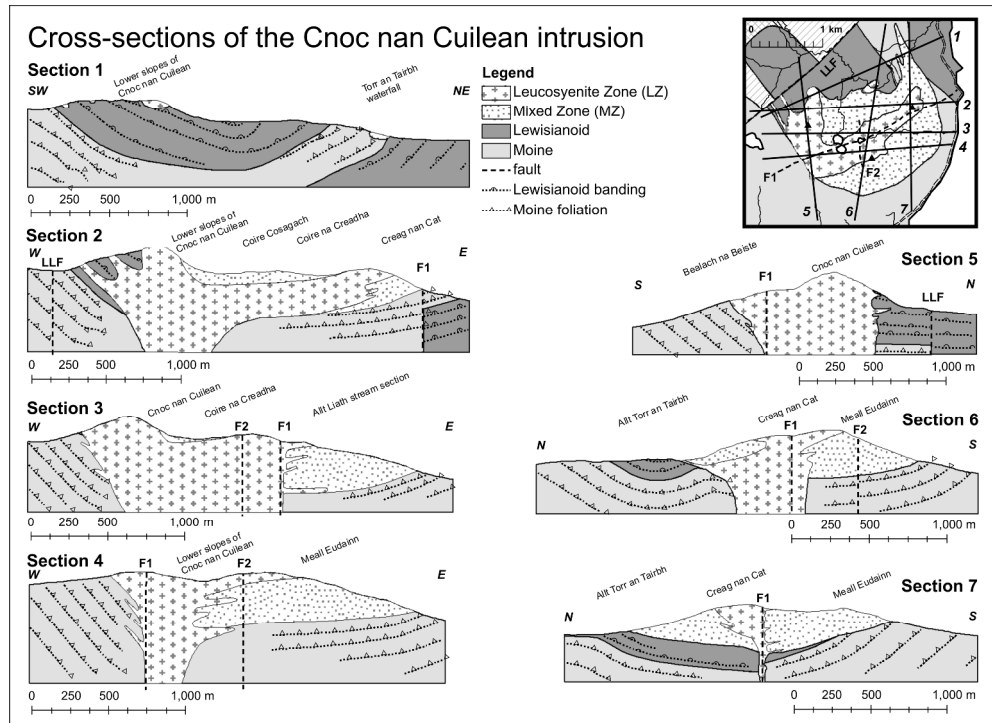


Figure 6. Cross-sections of the Cnoc nan Cuilean intrusion showing broad synform within the country rocks, into which the lopolith form of the MZ sits, overprinted by later intrusive events associated with the LZ. LLF is Loch Loyal Fault, F1 and F2 are Faults 1 and 2 respectively, within the Cnoc nan Cuilean intrusion.
165x118mm (600 x 600 DPI)

review

1
2
3
4
5
6
7
8
9
10
11
12
13
14
15
16
17
18
19
20
21
22
23
24
25
26
27
28
29
30
31
32
33
34
35
36
37
38
39
40
41
42
43
44
45
46
47
48
49
50
51
52
53
54
55
56
57
58
59
60

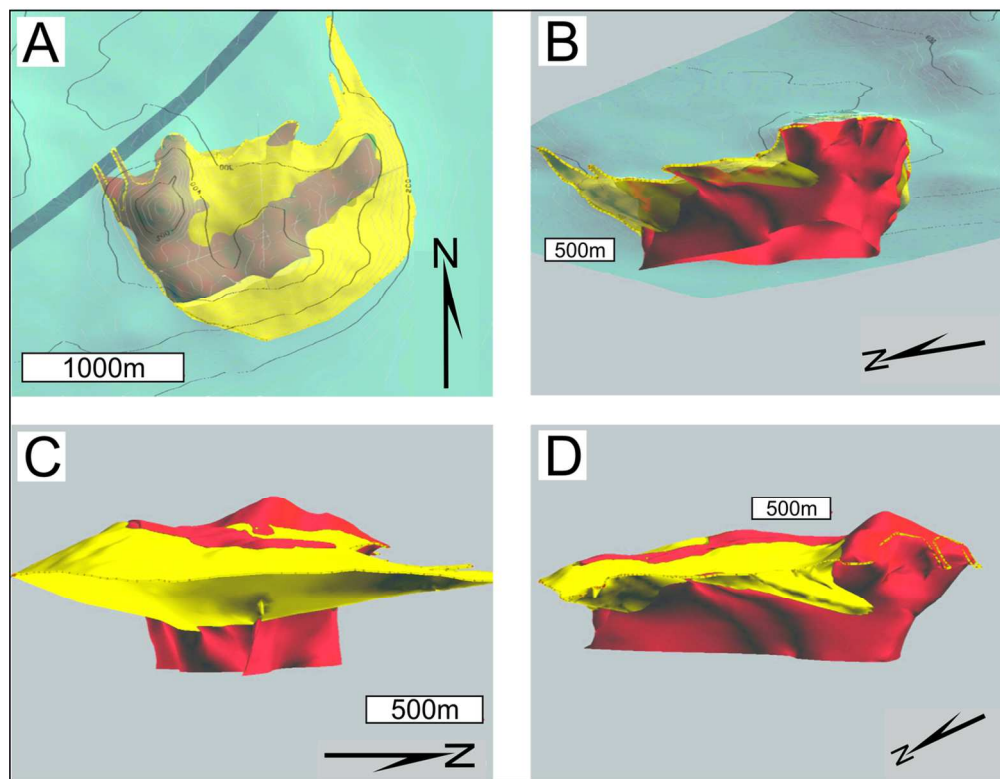


Figure 7. (Colour online) Snapshot views of the 3D GoCADTM model of the Cnoc nan Cuilean intrusion. (a) Plan view of the intrusion showing contoured topographic surface. (b) View from beneath the NW corner of the intrusion. (c) View from E of the intrusion, demonstrating the lopolith shape of the MZ and more elongate vertical body of the LZ (white line indicates ground level of the margin of the intrusion). (d) View from N of the intrusion. MZ is the yellow body (or lighter grey in print), LZ is the red body (or darker grey in print).

123x98mm (300 x 300 DPI)

ew

1
2
3
4
5
6
7
8
9
10
11
12
13
14
15
16
17
18
19
20
21
22
23
24
25
26
27
28
29
30
31
32
33
34
35
36
37
38
39
40
41
42
43
44
45
46
47
48
49
50
51
52
53
54
55
56
57
58
59
60

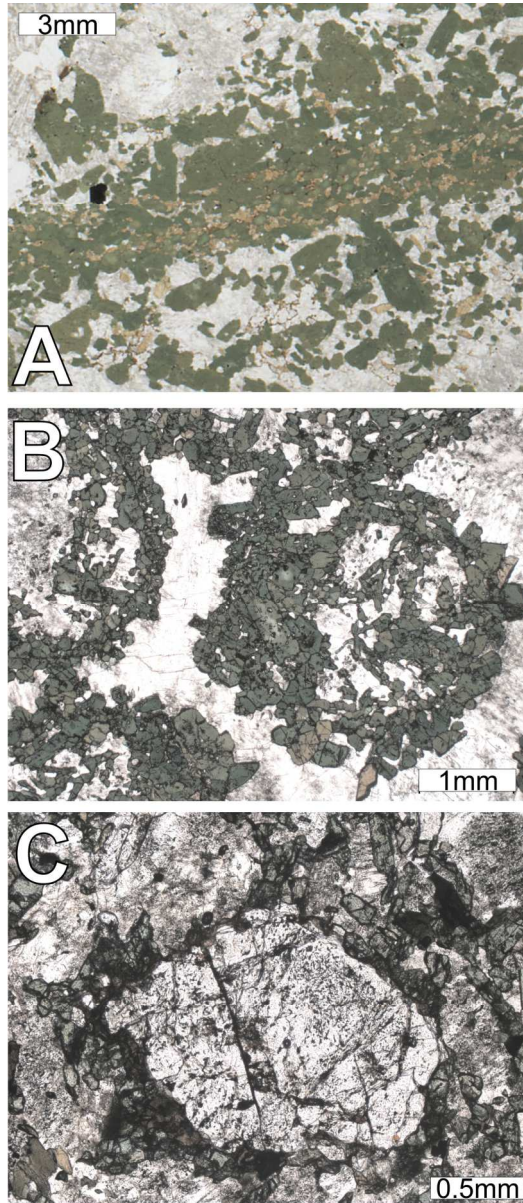


Figure 8. (Colour online) Photomicrographs of textures for syenites. (a) Clustered clinopyroxene, titanite, and apatite in melasyenite stringer. Fine dark brown allanite interstitial within this stringer. Coarse perthitic K-feldspar either side of mafic mineral stringer. (b) Example orbicular texture in melasyenite, with green clinopyroxene, amphibole, and titanite forming rounded clusters between coarse K-feldspar crystals. Orbicule centres also with coarse perthitic K-feldspar. (c) Coarse rounded apatite crystal (from melasyenite) with a partial allanite rim and surrounded by K-feldspar (with albite exsolution) and prismatic clinopyroxene. Apatite is inclusion-rich (often magnetite flecks) with allanite infilling fractures.

174x400mm (300 x 300 DPI)

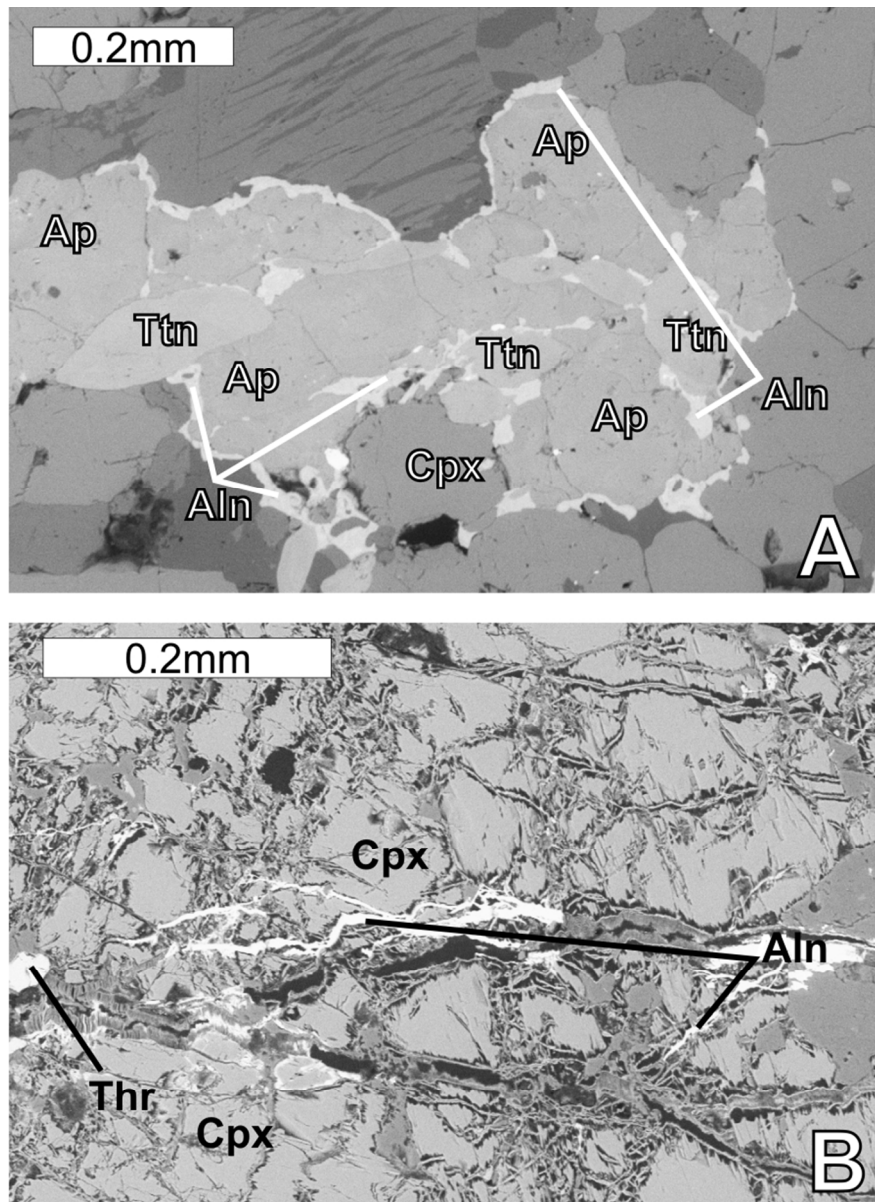


Figure 9. Selection of Scanning Electron Microscope Back Scattered Electron images of samples from the Cnoc nan Cuilean intrusion. (a) Interstitial allanite between euheedral and subhedra clinopyroxene, titanite, and apatite (with K-feldspar and albite exsolution lamellae in top of view) in melasyenite. (b) Allanite infilling fractures through coarse clinopyroxene crystals within melasyenite sample. Bright thorite also seen as rounded crystals infilling vugs or fractures. Mineral abbreviations: apatite (Ap), clinopyroxene (Cpx), titanite (Ttn), allanite (Aln), and thorite (Thr).
75x103mm (300 x 300 DPI)

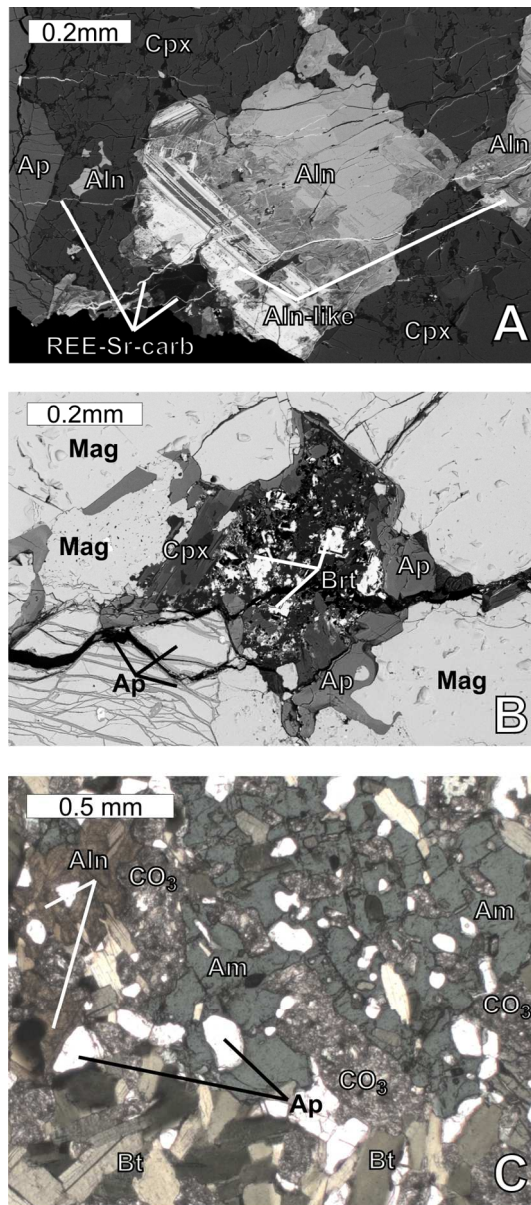


Figure 10. Scanning Electron Microscope Back Scattered Electron image of biotite-magnetite vein material showing (a) allanite with an allanite-like banded mineral and (b) baryte, thorite, and apatite infilling a large vug within a fractured magnetite crystal. (c) Photomicrograph of a metasomatised melasyenite sample exposed adjacent and external to biotite-magnetite veins. Poikilitic amphibole has abundant inclusions of apatite, while small tabular biotite and cryptocrystalline carbonate replace and overprint the original feldspar component of the syenite. Mineral abbreviations: apatite (Ap), clinopyroxene (Cpx), amphibole (Am), biotite (Bt), titanite (Ttn), allanite (Aln), allanite-like mineral (Aln-like), magnetite (Mag), thorite (Thr), baryte (Brt), REE-Sr carbonate veining mineral (REE-Sr carb), and carbonate (CO₃).

75x170mm (300 x 300 DPI)

1
2
3
4
5
6
7
8
9
10
11
12
13
14
15
16
17
18
19
20
21
22
23
24
25
26
27
28
29
30
31
32
33
34
35
36
37
38
39
40
41
42
43
44
45
46
47
48
49
50
51
52
53
54
55
56
57
58
59
60

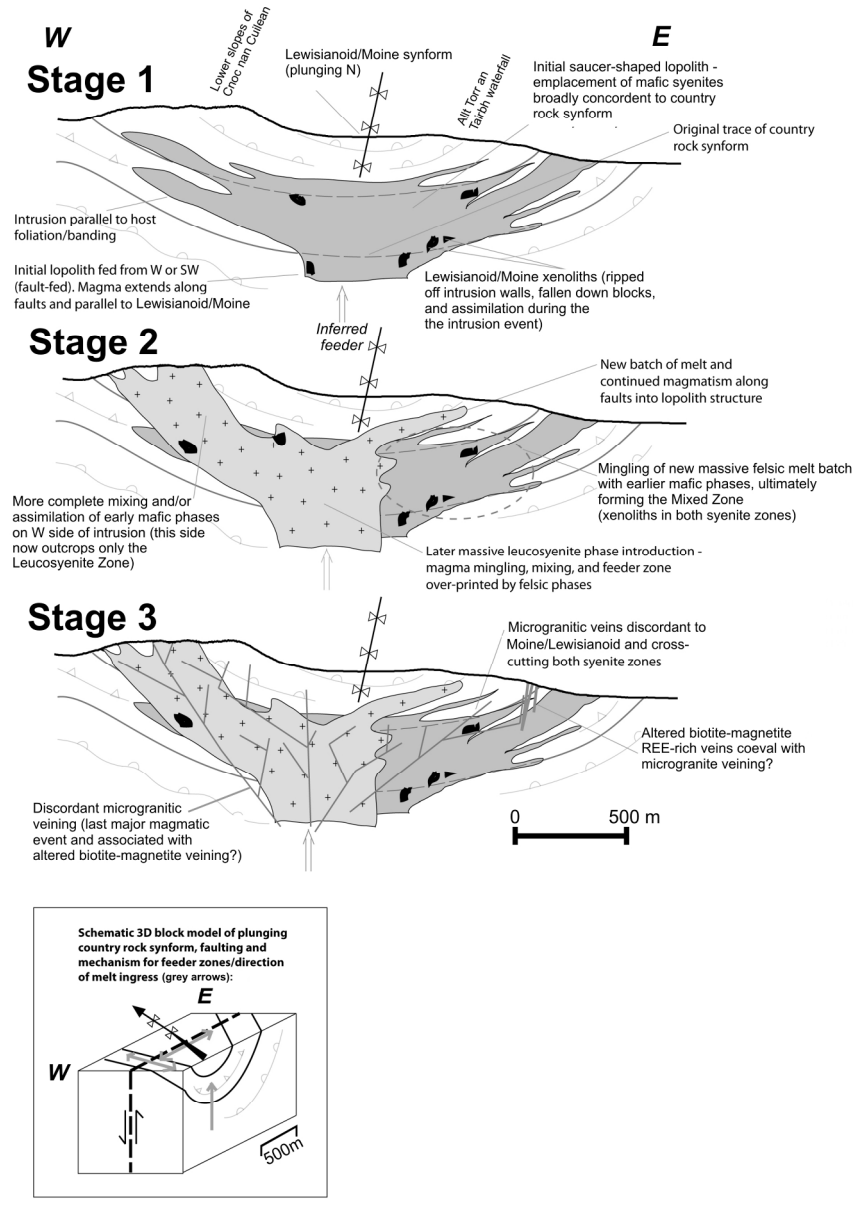


Figure 11. Schematic diagram demonstrating the formation events of the Cnoc nan Cuilean intrusion. 170x227mm (300 x 300 DPI)